THE PENNSYLVANIA STATE UNIVERSITY
SCHREYER HONORS COLLEGE

SCHOOL OF SCIENCE, ENGINEERING, AND TECHNOLOGY

A STUDY OF STIFFNESS IN CONTROL ARMS UTILIZING INNER WEBBED STRUCTURES TO MINIMIZE DEFLECTIONS

JAMES ANDERSON
Spring 2014

A thesis
submitted in partial fulfillment
of the requirements
for a baccalaureate degree
in Mechanical Engineering
with honors in Mechanical Engineering

Reviewed and approved* by the following:

Amit Banerjee, Ph.D.
Assistant Professor of Mechanical Engineering
Thesis Supervisor

Issam Abu-Mahfouz, Ph.D., P.E.
Associate Professor of Mechanical Engineering
Faculty Reader

Ronald Walker, Ph.D.
Associate Professor of Mathematics
Honors Adviser

* Signatures are on file in the Schreyer Honors College.

ABSTRACT

Millions of vehicles traverse our roads every day and automobile safety is ever more important. Automotive control arms are an essential component of a vehicles suspension system and their design and construction can directly affect vehicle safety. The purpose of this thesis is to evaluate control arm deflections and if using a specific cross sectional shape for a machined inner structure, determines the increase in stiffness of aluminum control arms. Aluminum control arms made from a 6061 alloy, utilizing a machined inner bracing were manufactured and tested until failure occurred. Various control arms were machined each using a different cross sectional shape as the bracing which composed the inner webbed structure. The arms were then strategically tested and monitored to determine if stiffness can be reliably improved. Using a specially designed jig and a universal testing machine the arms were individually subjected to a steadily increasing load at the tip of the control arm. Using a Linear Variable Differential Transducer, strain gages and the tensile tasting machine's computer interface the deflections, load and stresses were recorded and monitored for comparison.

The results will provide a determination that a specific cross sectional shape can be used to better increase a control arms resistance to deflections. The thesis provides an in-depth study of deflections in planar control arms to be used by automotive engineers. The results are particularly interesting to light weight sport compact, hybrid and racecar suspension designers. The experimental results in some cases compared favorably with the associated FEA simulation results. Although, the numerical values did not agree, the general trends were consistent in both the experimental portion and the FEA Simulation.

The patterns were similar and consistent considering there was an acceptable amount of experimental error. The results proved that some cross sectional shapes used in the bracing members performed better in certain situation. It was found that decreasing the amount of deflection in the test specimen was more so dependent on the trajectory of the cross bracing. The bracing trajectory had a larger influence on the associated deflection than the cross sectional shape of the bracing itself. It was also observed, that in some trajectories of the cross bracing the load at which the specimen failed changed very little in comparison to the unbraced arm. However, the associated deflections varied quite drastically.

TABLE OF CONTENTS

LIST OF FIGURES

LIST OF TABLES

ACKNOWLEDGMENTS

Throughout the course of this project, I received support and assistance from numerous individuals. I would like to take this time to mention a few individuals who were of extra importance to the completion of this project. These people devoted much time and energy into helping guide me through this project from beginning to end.

I would first like to thank Dr. Amit Banerjee. Thank you for your time and willingness to work with me on a regular basis. You were of great assistance in many ways, not only as my thesis supervisor but was a key contributor to the outcomes of this study. Your devotion to helping me towards a successful completion is admirable. It was an honor to be able to work with you. You have helped me to develop many skills that will follow me throughout my lifetime as well as aid me in being a valuable member of the work force. You devoted numerous hours of your personal time and for that, I am extremely grateful.

I would next like to thank Dr. Issam Abu-Mahfouz. Thank you for your time and persistence in helping me throughout this project. You have provided me with much assistance in during the course of the project. You donated more help and time than what was expected. Your perseverance in helping me to obtain good quality and reliable data was beyond expectations. I am thankful for having the opportunity to work with you and be able to learn from your expertise and experiences.

Additionally, I would like to thank Drs. Ronald Walker and Oranee Tawatnuntachai. These two have provided me with much needed guidance during the foundational stages of this project. You have been of especial importance during the written portion of my thesis and I am grateful for all of the time you spent helping me improve my work.

I would like to thank Mr. Robert Krick of KB Systems Inc. You have been especially important to the success of this project. Your willingness to donate your time and energy into water jetting the required parts for this thesis saved countless hours of machine time and programming. The costs saved by your services made this project possible. You have been great friend for many years and will continue to be for many more. Friends like you are hard to find and only come once in lifetime. Thank you for your support and assistance.

Lastly, I would like to thank my family and friends who have never stopped supporting me. You have all been there for me during the course of this project as well as my college career. I would also like to recognize two great men in my life who passed away during the course of my college education, my grandfathers, Jim Anderson (December 2012) and Bill Muth (March 2014). You guys have helped me stay focused and pushed me to never give up on my dreams. You will always be in my heart and I miss you greatly.

Chapter 1: Introduction

1.1. Introduction to Control Arms

In modern automobiles, the control arm is one of the most important components of a vehicles suspension system. Excluding heavy-duty work vehicles and a limited number of other select vehicles controls arms are present on just about every vehicle we encounter. Control arms can vary greatly from vehicle to vehicle but are generally identical in their purpose. They vary in shape, size, material and even the processes in which they are formed and manufactured. Each control arm material and method of manufacturing has specifics advantages and disadvantages. At this point in time, there is no mutually agreed upon ideal control arm. This is evident by a simple evaluation of vast number of different control arms that can be found on the vehicles.

Industry leading automobile manufacturers have not been able to agree as to which configuration of automotive control arm is best. This is primarily because there are essentially an infinite number of possibilities as to how a control arm can be produced. A control arm can be made in many different configurations and of various materials while still achieving the same desired capabilities. Even with the many advances in engineering practice control arms are still being designed as they have been for many years. The current approach is to design the arm to meet the desired objective only. This often leads to control arms that are far more robust than what is required to perform as needed. Optimizing the designs of future control arms will allow for stronger lighter arms.

With increasing environmental concerns and costs of fuel, it is becoming more important to maximize the performance and efficiency of today’s vehicles. One way in which performance and fuel economy can be improved is by decreasing a vehicles weight. Colin Chapman a famous automotive design engineer, and founder of the *Lotus* automobile company, said, “Adding power makes you faster on the straights. Subtracting weight makes you faster everywhere". This quote has gained momentum and is echoing even louder than ever before. In simple physics, Colin Chapman could not have been more right; if his famous quote were to be restated today it would probably contain some segment related to efficiency.

1.1.1 Control arm Function

Despite the variations and complex geometries that can be associated with vehicle control arms their function and purpose are relatively simple in nature. The control arm is just one of the many suspension components that make up a vehicles suspension system. It is responsible for positioning the wheels in the desired location and orientation. Vehicle suspension systems may contain or utilize multiple control arms per wheel. Each arm works to position the wheel by use of a ball joint in coordination with the vehicles steering knuckle. The control arm fixes the movement of the wheel in the wheel well by only allowing it to translate vertically. It constrains the motion of the wheel by not allowing it to translate horizontally with respect to the ground. The diagram shown in Figure 1 is one of many suspension configurations, however: it is useful in depicting the way a control arm is used in a vehicles suspension system.

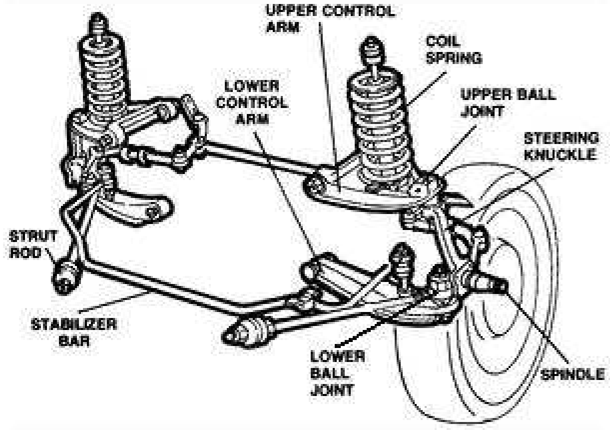

Figure 1 - Diagram of a Vehicle Suspension

The steering knuckle attaches directly to the wheel of the vehicle. The control arms orient and limit the movement of the steering knuckle which in return limits the movement of the wheels. All of these components are crucial to the vehicles ability to provide suspension and maneuver efficiently. Suspension components are subject to many harsh conditions as well as experience many types of loading. The suspension system is of the most importance in a vehicle because it maintains controllability. Being able to control a vehicle is important for the safety of anyone who comes in contact with them.

1.2 Thesis Overview

This thesis focuses on evaluating effects of adding bracing members to the interior of common planar control arms affects their resistance to deflections. The study evaluates the possibility of constructing aluminum control arms with mechanical properties comparable to those of steel arms. The arms are studied by both Finite Element Analysis (FEA) and experimentally. The specimens evaluated consist of a 1020 steel arm, which served as the experimental control, and various configurations of the same arm made of aluminum. The aluminum variations utilized interior bracing members with various common cross sectional shapes. The path of the bracing was initially chosen arbitrarily to evaluate the effects of the different cross sectional shapes.

Later the arms were studied again using the same shapes but altering the path of the bracing. The path for the bracing in both circumstances was chosen somewhat arbitrarily. The path and shape combination was studied again, monitored and compared to the previous arms as well as the control specimen. During the evaluations the stresses, strains, and deflections were monitored in both the FEA and the experimental portion.

Chapter 2: Literature Review

2.1. Introduction to Automotive Control Arms

In the modern automobiles of today control arms are one of the most important components of the suspension system. The primary function of a control arm is to hold the vehicles wheels in their desired location while hinging and absorbing the wheels vertical movement. In automobiles, the driving comfort and handling qualities are directly affected by the suspension system [1]. As designers struggle to meet consumers' expectations for comfort and efficiency the task of designing effective and reliable control arms is becoming increasingly daunting.

2.2. Control Arm Materials:

Automotive control arms can be safely constructed from many different materials; however, to maintain vehicle rigidity as well as meeting driver expectations Aluminum and Steel have prevailed as the most desirable materials to be used. These two competing materials are desirable because of their specific properties and practicality. The properties as well advantages of each of the materials will be further discussed in this chapter.

2.2.1. Aluminum

Aluminum has many unique properties that differ greatly from steel. Despite these differences, the materials do have a few minor similarities. Each of the materials can be incredibly strong depending on the alloying agents used in their chemical makeup. Aluminum has a large variety of specific alloys each with properties similar to pure aluminum but other properties that are alloy specific. Knowing the exact mechanical properties and uses of an alloy is essential in developing a control arm design. The mechanical properties of a 7075 aluminum alloy are some of the most desirable in control arm design, and closest in comparison to mild steel, which is the most commonly used material in control arms. 7075T6 aluminum alloy because of its alloying elements has fatigue strength close to that of steel [2].

Many of aluminum's material and mechanical properties can be altered by addition of specific alloying agents and treatments. Aluminum when alloyed with silicon has shown to have a significant increase in fatigue strength as well as a reduction in fretting wear [3]. Anodizing, a common surface treatment, when used with aluminum alloys showed to improve fretting wear resistance to be better than medium carbon steels when tested at 1 million cycles [4]. 6061M6 aluminum when used as an upper control arm, designed by optimizing the use of material, proved to be as strong as a steel counterpart and 16% lighter [5]. On the contrary, the upper control arm is typically subjected to compression forces and does not experience the large tensile forces that the lower control arm is subjected to. The lower control arm is more likely to fail as result of fatigue than is the upper control arm because of the loadings it endures [5].

Most control arms made of aluminum are generally not as strong as steel control arms because of aluminum being a softer more ductile material. Aluminum control arm designs need be carefully inspected to avoid high stress areas [6]. In addition, a result of aluminum's relative softness compared to steel, fretting wear is a more serious topic of concern, and should be carefully considered when designing a control arm and associated components [6]. Fretting is the wear or reduction in strength of a component due to the friction and continuous relative rubbing motions between two entities. Despite increased concerns, aluminum can still be used in control arms though a more thorough design process is required [1].

2.2.2. Steel

Steel is one of the most widely used metals and has been the industry standard in control arm construction. Steel has seen use in almost every application imaginable. It has many good properties such as being inexpensive, extremely hard, and quite strong and comes in over 100,000 unique varieties. Some disadvantages of steel are its weight, natural tendency to oxidize and formability. Using 3D modeling software designers can still meet the demands for lightweight and strong suspension components made from steel [7].

Due to steels material properties, it produces some difficulties in forming and manufacturing of parts. Despite difficulties in forming and manufacturing steel can still be used to produce lightweight, strong and effective control arms. Some of the most crucial difficulties associated with steel are encountered when press forming parts from blank steel sheets [7]. The press forming process creates areas of high stress. In response to the issues associated with press-formed steel control arms there are methods that can be used to reduce these highly stressed areas [7], [8]. Surface treatments and electrochemical analysis methods can be used to analyze and improve fatigue life [8].

Being familiar with material processing techniques and treatments relevant to steel can offer the designer a larger selection of alloys to choose. This is especially important when designing for infinite fatigue life. As with aluminum, although not as severe, fretting is still an issue of concern when designing with steel [9]. Fretting wear on steel control arms can be significantly reduced by the use of surface treatments. After an initial bed of debris is created by the wearing surfaces fretting is decreased [3], [9]. In addition to traditional dry wear contact, changes in the level of fretting wear occur depending on environmental conditions and temperature [9].

Steel control arms have shown to experience heightened stress levels in the areas located near arc-welded components [10]. Being that welding is a typical method used in manufacturing of steel products it is essential for designers to anticipate the reduction in fatigue life after welding. Welding should be avoided if possible because not only does it form weak spots, it also results in discontinuities and uneven distributions of alloying elements near the welds [10].

2.2.3. Material Treatments

Both materials discussed in this section have numerous treatment methods and techniques to improve or alter their characteristics to be more desirable for designers. These treatments and processes have effects on the molecular level and can dramatically change the mechanical properties. Attempting to weld or fuse aluminum alloys or other non-ferrous metals causes disruptions in the materials matrix and an undesirable distribution of the alloying elements [4]. This also agrees with the results of arc welding steel components [10]. To avoid these disruptions in the material welding should be avoided and fasteners should be used to join pieces if they cannot be formed as one unit [4].

Joining components by fasteners may cause fretting, however; if done properly the effects will be less than those caused by welding [4]. Based on experimental data, addition of silicon as an alloying agent in aluminum can decrease fretting. Silicon not only showed to increase fretting wear resistance but when alloyed at 20% silicon by volume, fatigue strength was increased. In addition to these results, similar conclusions based on experimental data can be made [3], [4]. By anodizing the 20% silicon based aluminum alloy the fretting wear was even further reduced, even after 1 million cycles [4]. Contact of sliding surfaces formed initial wear and debris between the materials. The bed of debris formed by the wearing surface treatments and the large silicone particles in the aluminum alloy together created a natural lubricant reducing the effects of fretting. Steel samples were also found to have similar results and lower levels of fretting wear when surface treatments were applied. The treatments applied need to be varied depending on the specific alloying agent used [8].

Although steel is typically harder than most aluminum alloys and more resistive to fretting wear, some aluminum-silicon alloys with anodized surfaces showed to be more resistive to fretting than steel [4]. Fatigue and tensile strengths can be increased by alloying aluminum with scandium and zirconium [11]. Alloying aluminum with scandium and zirconium showed desired increases in material properties such as fretting wear resistance and hardness [11]. On the contrary, when an aluminum sample was sprayed with a scandium and zirconium solution the effects were opposite and caused reductions in mechanical properties [11].

2.3. Control Arm Failure Analysis:

Automotive control arms are subjected to a variety of loads. Understanding the loading conditions and the modes of failure are crucial for design engineers. Control arms frequently experience deflections and deformations caused by impact loads. These impacts loads occasionally results in failure of the control arms, which will be discussed in this section.

2.3.1. Loadings and Deformations

Automotive control arms are constantly subjected to a variety of loading situations. Control arms often experience tensile stresses, compressive stresses and often impact and bending stresses. These combinations of stresses over long periods of time greatly reduce the strength of the control arms. The lower control arm on most vehicles generally endures the greatest stressors as well as the most severe loading conditions.

In order to properly design a vehicles control arms, designers need to accurately estimate the load conditions that an arm may be subjected to. Estimating the loading conditions is not only important for durability of the arm, but also essential to the calculation of expected control arm deformations. Control arms that deform and deflect under loading conditions can cause hazardous situations for the driver. Deflections of the lower control arms can greatly affect the ability for a driver to maintain control of their vehicle and steering ability is hindered [12]. Under hard breaking conditions, deflection of the lower arms can cause the vehicle to experience lateral drift and leave the intended path.

Proper simulations must be performed before choosing a material for both the control arms and the vehicles lower sub frame connection points. Despite the fact that all control arms will experience some degree of deflection it is ideal to minimize the distance in which it will deflect in extreme conditions [12]. In order to reduce the shock and impact loads that a control arm is subjected to solid rubber bushings are often inserted in to the control arm at multiple points of connection. This allows loads to be transferred to the body of the vehicle in a smoother less dramatic manner. These bushings often transfer the load as function of their stiffness and can have positive effects on fatigue life [13].

2.3.2. Fatigue

Fatigue is the number one cause of failure in all mechanical components. The cyclical loading which causes fatigue failure is common in most mechanical components so being able to analyze and estimate fatigue life of a design is essential. Fatigue strength is defined as the amount of stress, particularly von Mises stress, that a mechanical component can with stand for a desired number of times the load is applied. If a part is designed for infinite life, it is expected to withstand 1 million loading cycles. Fatigue life is calculated depending on the specific shape and size of the part. Fatigue strength is dependent on geometry and many other factors including the material to be used. Fatigue strength can vary greatly depending on the specific design. Fatigue is the most crucial factor to be considered in the design process.

It is possible to develop a control arm made of 7075T6 aluminum alloy that can reach the minimum required fatigue strength needed in control arms [2]. Fatigue failures result after microscopic cracks in the material experience growth due to the cyclical loadings they endure. This crack growth is referred to as crack propagation and is often assessed using many different techniques and various pieces of equipment. Some designers spend their entire careers studying crack growth and specialize in the area of fracture mechanics.

Fracture mechanics and predicting fatigue life becomes increasingly difficult as environmental conditions change. Despite the associated difficulties, a process has been developed to determine environmental effects on fatigue life. When a material is exposed to things such as steam, dry air, vacuum, and elevated atmospheric pressures, fatigue life can be significantly reduced. A Scanning Electron Microscope (SEM) can be used to analyze the environmental effects and the associated crack growth in most materials [14]. This approach is ideal; however, it is only relevant for small parts. As discussed previously small disturbance such as fretting caused by pressed-in bushings can have a dramatic effect on fatigue life of control arms, especially in aluminum [6]. The decreases in fatigue life of aluminum due to pressed-in bushings is a result of the material being softer then the steel sleeve being pressed into it [6].

Fatigue life can also be dramatically reduced as a result of arc welding. Arc welding steel control arms reduces fatigue life by initiating microscopic cracks at the root of the weld [10]. Notches and other critically stressed areas can become severe weak spots when arc welding is used in their immediate vicinity. Understanding the effects of arc welded components is essential for engineers designing dynamically loaded steel parts. Many control arms are constructed from steel and require arc welding to properly join associated pieces. Arc welded control arms were found to have critical stress concentration factors as high as five in bending and three in axial loaded situations [10].

Fatigue life predictions for control arms can usually be made when careful considerations are taken, despite the inherent difficulties. Complex geometry along with dynamic loading situations increase these difficulties but the use of assumptions and various analysis techniques aid in simplifying fatigue life determinations [2]. The automotive industry has three widely used and accepted methods in determining fatigue stress. The three widely used fatigue stress analysis methods are Static Response Optimization, Frequency Response Optimization and Quasi-Static Response Optimization [15]. Each of these techniques has strengths and weaknesses that must be considered when choosing which method to employ.

Each method has an associated error in their outcomes which can be accounted for by using a multi-axial hybrid stress analysis technique [15]. This hybrid technique satisfies the industry demand for lighter, stronger and safer components while minimizing material usage by employing an optimization based algorithm for use in control arm design [15]. The technique will produce the most accurate estimations of fatigue life when used with finite element analysis while reducing any incurred errors.

In addition to the cyclical dynamic loads, vibrations can also contribute to fatigue failure [16]. Vibrations in automotive control arms are common and stem from a variety of sources. The biggest sources of vibrations in an automotive control arm are generated from road conditions and engine vibrations.

2.3.3. Critical Stress factors and fretting

Fretting is the failure of a component, which is caused by premature wear, resulting from direct contact of two or more materials. Critical stress factors are numerical values used in representing areas of high stress for computational estimations of fatigue life. Critical stress factors are primarily used for dynamically loaded mechanical components. As previously mentioned, welding has shown to cause critical locations where stress related failures are likely to occur. Areas where welding has been performed need to be carefully analyzed, welding creates dislocations in the material which form weak spots [6].

Fretting most commonly occurs in automotive control arms when bushings are press fitted. Frictional resistances between the surface of the control arm and the typically steel sleeved bushings cause wear and fretting while the two are being forced together.

Even though fretting affects are relatively small, disturbances in the material are formed and often lead to failure points. Bushing locations in many control arms, because of their changes in geometry, are naturally areas where concentrated stresses already exist. When these critical areas are combined with the additional stresses resulting from pressed fit bushings they often become the locations where failure will occur due to the increased pressure, strain and wear [6]. A remedy to fretting caused by press fit bushings is to shrink fit bushings into the control arm. This will avoid fretting wear and reduce material strains [6].

Attempting to weld or fuse aluminum alloys or other non-ferrous metals causes disruptions in the materials matrix and an undesirable alloy distribution. For these reasons the materials are usually joined by fasteners or adhesives which cause fretting [11]. Some common fasteners used in assembling control arms and their associated components are bolts, rivets and various adhesives. Subsequently, the best way to avoid these unwanted fretting situations, if possible, is for parts to be formed in one piece. Also, by addition of a silicon or scandium alloying agent fretting wear can be greatly reduced. A 2124 aluminum alloy with 20% silicon by volume showed better fretting wear resistance than some medium carbon steels when tested to 1 million cycles which is considered to be infinite life. As previously mentioned surface treatments such as anodizing up 20um thick significantly improves wear resistance even after the anodized coating has rubbed off [11].

During the sliding contact between surfaces utilizing various anodized surface treatments debris is formed. This debris forms a bed in which the two materials now slide. The bed of debris acts as a lubricant and actually reduces fretting wear and frictional resistances when compared to components which do not have surface treatments [3]. Fretting wear in aluminum alloys can be decreased by a variety of anodized surface treatments as well as by the addition of silicon particles as an alloying agent. Similarly, the addition of 3um silicon particles in .4% carbon steel showed to increase fatigue strength up to 50% and improved fretting wear resistance [3]. This agrees with the conclusion that an anodized surface coating up to 20um thick will improve fretting wear on aluminum alloys [11]. These results also agree with a study showing that initial fretting wear on mild steel is significant at first but is greatly reduced after a bed of debris is formed between the surfaces [9].

It can be concluded that fretting wear on a variety of surfaces and materials is most significant during the initial wear. After an initial bed of debris is formed fretting wear is decreased considerably. In contrast, control arms are frequently subject to temperatures both above and below room temperatures as reported in previous articles. They can often experience higher localized temperatures due to use in warmer climates and excessive heat generated by breaking components. In high-performance vehicles this becomes more significant and deserves an investigation [17].

2.4. Control Arm Components:

Control arms are an important component of a vehicle’s suspension system; however, they do not function entirely on their own. Control arms often have additional components associated with them. The components allow for proper operation of the control arm while aiding in performance. These essential components improve the suspension system as a whole, but occasionally have lasting effects on the control arm itself. The interaction between control arms and their associated components is discussed in this section.

2.4.1. Ball joints

In control arms, ball joints are one of the most important components. Control arms incorporate ball joints as an essential component aiding to their functionality. The ball joint is a relatively simple component which is occasionally bolted or riveted in to the control arm. Most times when a control arm houses the ball joint, it has been pressed into a collar in the control arm. The collar which holds the ball joint can be machined, forged or casted with the arm itself. This collar is usually an area where stress concentrations will occur. Since the ball joint is located at the end of the control arm which attaches to the steering knuckle and wheel hub assembly it is typically the point where the greatest loads are applied. Loads generated by the vehicle's weight and tires in contact with road surface, make up the dynamic loads that the joint is subjected to.

Ball joints can swivel and rotate while handling significant loads and that makes them desirable for use in vehicle suspension systems. In some suspension systems the ball joint is located in the steering knuckle assembly and the attaching or threaded end of the joint is bolted into the control arm itself. In either situation, the control arm experiences fretting and fretting wear as a result of the ball joint's presence. In most cases ball joints experience failure before control arms do. The reason for this is because as part of their design they incorporate some areas with large critical stress concentration factors [18]. The joints fail due to the fatigue they experience from the cyclical loading on the suspension system. Ball joints with lower critical stress concentration factors can allow for more reliable operation of joint and increased fatigue life.

2.4.2. Bushings

As previously mentioned, control arms generally include the use of at least one or more bushings as essential components. Bushing help to reduce road noise, improve comfort and vehicle control by absorption of vibrations. Bushing aid in reducing the transfer of sudden shock loadings generated by road conditions directly to the control arm. The use of bushings generally improves fatigue life and reduces strains in the control arm. The stresses imposed on the arms by the bushings do not constitute a linear relationship with the applied loads that are generated by the road [13].

The stresses control arm's experience at their bushing locations vary significantly depending on the driving conditions. Bushing can cause fretting wear and decrease fatigue strength not only during press fitting but also under normal use [7], [13]. Bushings are generally exposed to rotational and translational stresses which can have effects on the control arm which they reside in [13]. Fortunately, there is an analytical algorithm which has been developed to address these stresses. These algorithms can be used during the design process along with the coefficients of elasticity of the rubber bushings to be used to estimate control arm stresses at bushing locations.

2.5. Control Arm Design Analysis:

Control arm designs need to be evaluated before production can occur. Design analysis can be performed by hand, however; the analysis can become very cumbersome for complex designs. Analysis is usually performed using 3D modeling software packages with finite element analysis capabilities. These software packages dramatically reduce the work required in analysis and often times provide extremely accurate results.

2.5.1. Finite element analysis (3D)

Design engineers often use 3D finite element analysis methods to evaluate product designs that utilize complex geometry. It is more efficient for design engineers to take advantage of 3D modeling software with finite element capabilities rather than performing physical experimentations. There is a variety of modeling software packages that are typically used by engineers. For instance, Solid Works is common software that is used to analyze the fatigue stresses and dynamic loadings that control arms are subjected to. The dynamic loading conditions are generated using collected data from a vehicle testing facility. The software allows for the critical stress points to be determined and altered for improvement. Solid Works offers some particular design optimization techniques and has the capability to generate mathematical models [1]. Another common 3D modeling software which incorporates a finite element analysis tool is Pro-Engineer.

Optimization techniques can aid the design process by reducing costs as well as improving part reliability. The optimization methods can also help to improve vehicle ride characteristics related to control arm design in specific applications. Similarly, 3D modeling software packages are also used in optimizing the manufacturing process. Modeling software can offer possible solutions and techniques to improve manufacturing processes as well as provide an increase in quality control to ensure the parts are manufactured to tight standards. There are established methods of using 3D modeling software to analyze and identify critically stressed areas that occur during a variety of manufacturing processes such as stamping or forming processes [7].

An optimally designed aluminum control arm can be made that is equally as strong as one previously made of steel. This is achieved by employing a variety of computer aided design techniques to minimize the material used and analyze the stresses involved. The weight of control arms can be reduced by 16 % when using an optimally designed aluminum arm (compared to steel) [5]. Optimization has shown to improve both ride control and establish aluminum arms with fatigue strengths comparable to their steel counterparts. The use of engineering design and optimization software enhances product design and analysis. This ultimately allows for lighter, stronger and more effective control arm design.

2.6. Control Arm Manufacturing:

Manufacturing of automotive control arms can be done in a variety of ways as well as from a wide array of materials. The most common manufacturing techniques include casting, machining and stamping. Previously control arms were generally constructed of steel only. With the ever-changing automotive market, manufacturers are now pushing towards constructing control arms from aluminum alloys. Aluminum alloys can exhibit mechanical properties close to those of steel at a fraction of the weight. This section focuses on the two most widely used materials and the specifics of their forming.

2.6.1. Steel

Steel control arms can be manufactured in a variety of ways. Some of the most common control arm production methods include, press forming, casting and machining. Machining steel control arms is the least common method of the three. This is because of the inherent difficulties associated with the use of steel as well as the time required for machining. Machined steel arms are generally made to the highest standards and can be made very accurately. The other two mentioned methods are far more common because of the ability to mass produce many arms very quickly. The press forming or sometimes referred to as stamping method to manufacturing control arms stamps out and forms control arms from steel sheets. This technique can form and manufacture high strength yet lightweight steel control arms fast and consistently. This method of manufacturing has shown to meet the demands for lightweight suspension components while maintaining high quality and high strength [7].

Despite the popularity of the press-forming method it has some limitations. Press formed steel control arms, depending on the complexity of their geometry, can develop cracks and significant strains due to the material deformation during the stamping process. Despite difficulties, there are solutions and techniques to improve the process as well as increase quality control to ensure stamped parts will be manufactured as desired. An issue not directly related to the stamping process is that of welding. Many times stamped control arms require some degree of welding in order to join the stamped parts. As mentioned before welding has shown to cause undesirable disturbances in the material, which is something designers must take into consideration [7].

Casting of steel control arms is another popular method, which also has some limitations as well. It is difficult to cast parts with complex geometry so casted control arms are generally simple in nature. Casted control arms are typically quite heavy and this method is sometimes undesirable for that reason alone. Casting steel control arms is also and much less efficient method of manufacturing compared to stamping or press forming. Casting steel control arms also requires a significant investment of capital and consumes more energy than other methods. Despite the down sides of casting control arms, it is still common because the method allows for consistent parts that are generally stronger and not pre-stressed as is common with some other methods.

2.6.2. Aluminum

Aluminum control arms are often manufactured using the same methods as those used in steel control arm production. The only difference is that stamped or press formed aluminum control arms are not very common. The most common method to forming and manufacturing aluminum control arms is casting because it can be performed quickly and easily. Also, being that aluminum melts at much lower temperatures than steel it can be casted much more efficiently and requires considerably less resources. As mentioned before aluminum cannot with stand very large internal strains and stresses like steel can so press forming is not desirable. Machined aluminum control arms are very popular among high-performance vehicles and race cars. This is because they can be made very precise as well as strong and lightweight. Machining aluminum control arms is often considered the best method to use for industries or applications where time and money are not of the biggest concern. For everyday consumer vehicles, machining control arms is not desirable because it costs considerably more and is time consuming when compared to other methods.

As with steel control arms steel sleeved bushings still need to be pressed into the aluminum control arms which cause issues of fretting. Like steel control arms, these issues may be overcome by shrink fitting bushings into the control arm [6]. These pressed-in steel sleeved bushings become a significant cause for concern in aluminum control arms because of the inherent material properties. Although aluminum control arms can be manufactured to endure the same stresses and loads as steel arms they typically experience reduced fatigue life and increased crack propagation [6].

The most common method of aluminum control arm manufacturing is casting. Casting of aluminum though has some concerning issues that need addressing. During the cast forming process impurities often arise in the aluminum alloy and can cause variations in the material properties. There are direct relationships between the impurities of an alloy and its associated fatigue strength. Different forming processes allow for different impurities to be imparted in the metal causing inconsistencies [19]. Also porosity of the material also becomes of concern when casting aluminum alloys. Different alloying agents allow for varying porosities. Materials having increased porosity showed a significant reduction in fatigue strength. Certain alloying agents when casted tend to cluster at locations in the material and do not disperse uniformly, which causes weak spots in the material [19]. This reduces the certainty of the materials strength. Alloys with larger porosity and inclusions occurring at the surface of the material experience the most dramatic effects and reduce fatigue life by the largest amount.

Like steel, Aluminum has a wide range of available alloys, each with its own characteristics. Each of the alloys available has slightly differing mechanical properties and can undergo a wide range of treatments to improve or alter those unique properties. Aluminum is also sometimes preferable to steel because it can be easily recycled and reused to produce new products. Aluminum, generally speaking, can be machined twice as fast as steel and in some case, this is a desirable characteristic that can warrant the tradeoff between the two. Overall, aluminum has many desirable characteristics making it regular substitution for items currently made of steel.

Chapter 3: Materials and Methodology

The primary objective of the study is to determine if an Aluminum alloy control arm can be stiffened by using a machined web structure to reduce deflections caused by hard braking conditions. This study is important because deflections of control arms caused by hard braking conditions have been shown to reduce handling and can affect the driver's control of the vehicle. Deflections in control arms can contribute to lateral drift, causing vehicles to leave their desired path and enter lanes of opposing vehicles or deviate from the road entirely [4].

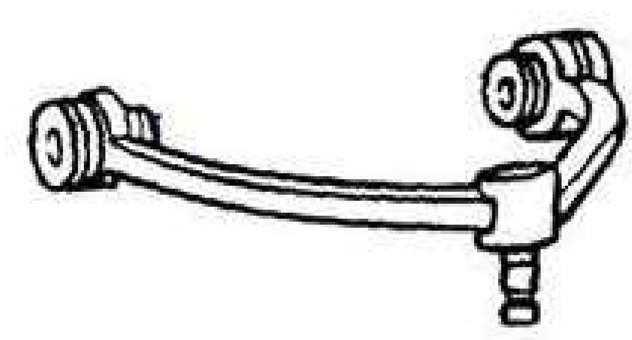

Figure 2 - Basic Planar Control Arm

3.1 Material and Experiment

For the experiments conducted in this study, a preexisting design of a steel control arm was scaled down to half of the actual size and machined from a 6061 aluminum alloy. The purpose of scaling down the control arm is to conserve material and minimize waste, as well as time devoted to precision machining. In addition, scaling allows for measurements that are more precise and simplifies the experiments in regards to construction of the testing apparatus that was used.

The experimentation portion of this study was performed in two phases. Phase I consisted of four initial control arms. The first three arms were designs utilizing machined web structures with different cross sectional shapes and the fourth was the original scaled down control arm design with no webbed structure. The web shapes included one square and a rectangle in two different orientations. The cross sectional area of each shape was held constant at $0.05in^2$ for each shape used. The trajectory of the machined bracing was chosen arbitrarily and kept the same for each part. The original scaled control arm served as the control for the experiment. Due to the high costs and difficulties of machining a steel control arm the study only focuses on the aluminum counterparts. However, the steel arm was compared in the finite element analysis portion of this study. The purpose of this part of the study is to establish a basis for comparison. The preexisting control arm design was analyzed using a finite element analysis to determine predicted deflections under heavy braking conditions. The scaled down manufactured control arms were then weighed and inserted into a specially designed jig. Using the jig, a steadily increasing static load was applied to the control arm to represent heavy braking conditions. The deflections and deformations of the control arms were monitored and measured continuously as the applied loads continually increased. The results from the experiment and the finite element analysis were compared to determine if they agree. The finite element analysis was then used to analyze more complex geometries and hard to manufacture cross section shapes such as a circle and triangle. These two shapes would ideally be studied experimentally, however; due to complexity of the CNC programming and the capabilities of the machines available it was decided that the simpler shapes would be used to validate the results obtained from the finite element analysis and then the same principles were carried over to the harder to machine parts. The original scaled down version of the steel arm was also analyzed using FEA as well due to limitations in budget and machining capabilities.

Phase II of the experiment consisted of analyzing the gathered data and observations collected from phase I. The results were used in determining which shape showed the greatest improvement in stiffness. The shape that produced the greatest improvement was then studied further by analyzing two more control arms with the same cross sectional area used in phase I. Only the trajectory was changed and again selected somewhat arbitrarily. The profile/trajectory in which the machined bracing follows was selected to utilize an ‘X’ shape because of the failure points that were identified in phase I. The results from these experimental parts were again used to validate the results shown in the finite element analysis. In addition, the trajectory was changed to show that the results can be applied to more than one configuration. The remaining shapes were studied using FEA only.

The finite element analysis of the testing fixture and control arm assembly showed that even a under a load of 4500lbs the fixture did not deflect or deform. The much weaker control arms deformed and deflected as desired. This confirmed that the fixture as designed would be extremely rigid and provide acceptable results. These results can be seen in Figure 3.

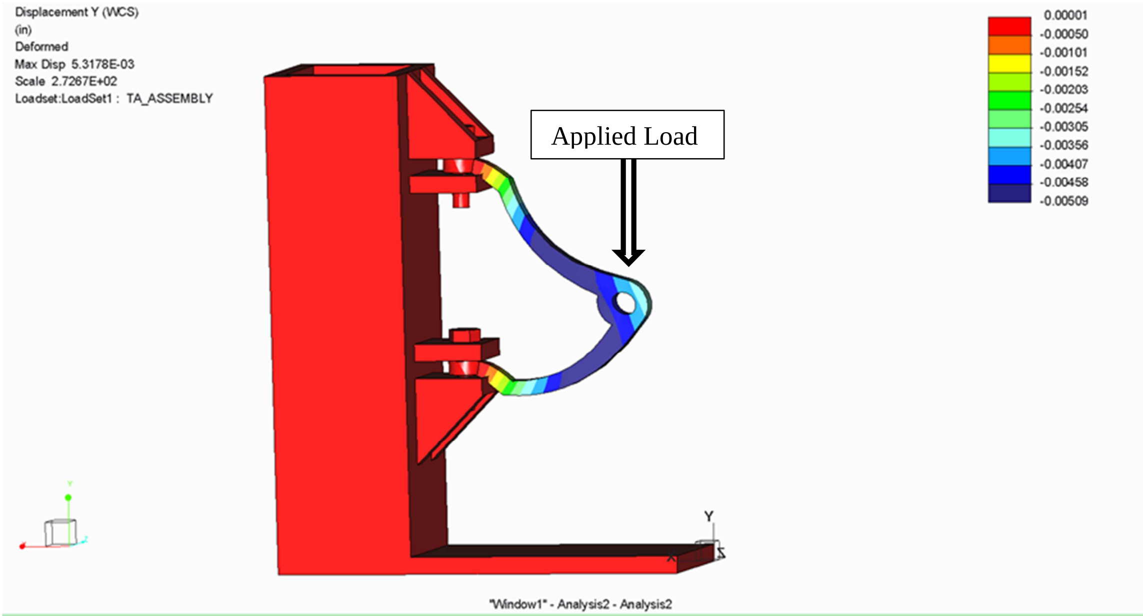

Figure 3 - FEA Study of Fixture and Original Arm Assembly

Each experimental arm was tested by installing it in the testing fixture and inserting the assembly into a Tinius Olsen Universal Testing Machine (UTM). The displacement of the arm was monitored through the use of a Liner Variable Differential Transducer (LVDT). The strains in each of the arms from the first stage of the experiment were monitored through the use of 4 strain gauges. The strain gages included one 45 strain gauge rosette and one single strain gauge. The strain gauges were positioned on the test specimen at exactly same location on each. This was performed in order to draw a comparison on the maximum principal strains in each arm at that specific location. The location for the gauges was chosen based on the results of the initial FEA of the arms. The mounting location on the arms showed to have the great maximum principal strains so the gauges were placed as close to that point as they could be. There were limitations on how close the gauge could be due to the size of the test specimen and interference from the fixture. The strain data was monitored and recorded using a P3 strain data acquisition box. Figure 4 shows the testing setup and procedure.

Figure 4 - Experimental Testing Setup

Each specimen was tested until complete failure which we defined as fracture of the specimen at any point or reduction in the load by greater than 25% of the maximum. The reduction in load criteria was set in order to define a stopping point for data collection in the test program. When an arm fractured the load would drop well below 25% of the maximum and therefore stop the test. In some cases the arms did not completely fracture but one or more of the bracing members did so, which allowed the load to drop below the maximum by 25% and the consequently ended the test for that specimen.

All of the control arm designs used in the experiments were first designed and analyzed using a 3D modeling software and finite element analysis. Following the finite element analysis of the designs, arms with the best performing cross sectional shape were machined from the proper materials and inserted into the same specially designed jig. The arms were then all tested in the same manner. Incremental static loads were applied to the arms and the strain, deflections and load applied were monitored and recorded. These test results were then compared to the finite element analysis as well as to the other designs and controls for the experiment. The respective weight of each arm was also recorded and taken into consideration for the purposes of fuel economy as well as material and manufacturing costs.

3.2 Process

A billet sheet of 6061 aluminum alloy was then purchased from a local metal supplier and cut into one inch thick 8”x8” blocks. Each of the blocks was then cut using a water jet to match the top view profile of the control arms. The use of the water jet saved a significant amount of machining time required and greatly reduced the complexity of the G&M codes used. Robert Krick of KB Systems Inc. in Bath, Pennsylvania performed the water jetting for this study.

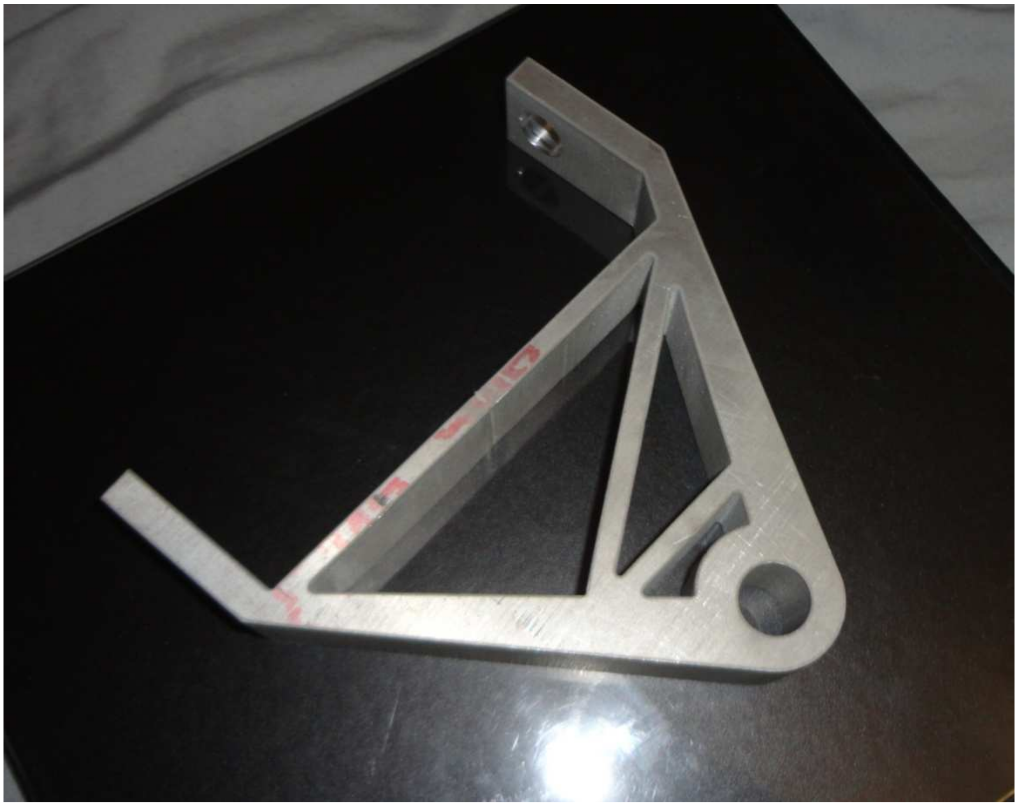

Figure 5 - Arms Post Water Jetting

The arms were then finally machined to their final dimensions using a HAAS CNC. Each control arm design was then tested at incremental statics loads while the force, displacement and strain data was simultaneously collected. A specially designed jig was created to test the arms and act as a representation of a vehicles sub-frame. The loads were applied using a Tinius Olsen UTM capable of applying a 200,000 lbf load.

Figure 6 - Arms at Various Stages of Manufacture

A program was written to perform the tests using the machine. The program directly monitored the force and the displacements occurring during the tests. The program was set up to measure the force internally and the displacement externally through the use of an integrated LVDT. The data was stored in the program's software and exported to MS Excel for analysis. The strain measurements were recorded independently using a P3 strain data acquisition box and software. The resulting data and measurements were recorded and displayed by charts and graphs in the results chapter. The data were compared against one another as well as to those of the finite element analysis.

Figure 7 - Square Arm during CNC Machining

In order to manufacture each of the test specimens and multistage manufacturing process was required. The profile for each arm was first cut out using the water jet as previously mentioned. The mounting holes were the arm would attach to a vehicle sub-frame were then drilled into the end of each arm. This can be seen in Figure 6 which shows the arms in various stages and clearly shows the mounting features being created. The arms then underwent several hours of CNC machining. The CNC machining was in itself a multistage process since the arms needed to be machined on both sides.

Figure 8 - Square Arm Post CNC Machining

3.3 Purpose

The experiments are designed to determine if control arms can be made stiffer against longitudinal deflections by employing a webbed center section. This study is being performed because little has been discussed among relative articles about deflections in control arms due to heavy braking conditions. Prior articles only observed that the deflections are present under harsh braking conditions and did little to addresses the correction of the resulting deflections. The study will be particularly applicable to lightweight sport compact vehicles, hybrids or a variety of racecars. For the near future, it is not anticipated that this will benefit the typical passenger vehicle directly because of the time consuming nature of manufacturing control arms in this manner. Based on current manufacturing techniques producing control arms in this manner is slightly inefficient and expensive although the high strength to weight ratios will ideally be utilized in specialty applications. The bracing, which is the same as the webbed center section of the arms, used has the potential to interfere with some common suspension systems although there are as mentioned applications in racing and other industries where this bracing would be desirable. Adaptation of competition style suspension systems such as those used in racing into passenger vehicles may allow for this style of control arm to become more widely used.

Figure 9 - Fixture Used for Testing

The testing fixture used to secure the control arms during the experiment was designed to be as ridged as possible and resist any deflections. The purpose of this was to provide a simplified model of a vehicle sub-frame. The fixture was constructed to represent a sub-frame that would not deflect under extremely heavy braking conditions. The arms were attached to the fixture through the use of a pin joint which was used in representing the bolts that constrain a control arm to a vehicle's sub-frame.

Chapter 4: Results and Discussion

In the first stage of the experimentation portion of this research project, computer simulation results were compared with actual experimental results. This included studying the testing fixture and a few of the control arms as an assembly. A load of 4500lbs was applied during the FEA analysis of the assembly in order to make sure the fixture would not deflect or deform during the experimental testing. Any deformation in the fixture would skew the experimental results.

In both stages of this study each arm was first studied by FEA. The results for each arm being studied in both stages are presented in the same manner. The stress of each arm was studied first by preforming a computer simulation and the results are displayed appropriately. Next a simulation of the maximum principal strains was performed and displayed as well. Additionally, the deformation of each arm was studied and displayed similarly. Lastly those arms which were able to be produced were constructed and tested experimentally. The results from the simulations as well as the experimental tests are displayed and discussed appropriately.

During the first stage, an arbitrary ‘Z’ shape trajectory was chosen and held constant for all parts. The trajectory was used to define the path in which the bracing of various cross sectional shapes followed. The purpose of this arbitrary trajectory was to validate that the addition of some cross bracing would decrease the deflections that occurred in a traditional unbraced control arm. This was also used to help determine if one particular cross sectional shape performed better than the others did. The cross sectional area of each shape used was kept constant at $0.05in^2$.

Based on the results of stage I it was determined that a stage II was necessary to further investigate the effects bracing members have on control arm deflections. The previously studied arms identified a common trend of failure occurring at a location close to the mounting holes. It was also observed during the FEA of the stress in each arm that the center member was being stressed significantly more than the other two. From these results it was determined that a new trajectory for the cross sections to follow was needed. The new trajectory was chosen to utilize and 'X' shaped pattern and evaluated to see if the same results occurred that were previously noticed. The new trajectory was chosen to attach to the outer elements of the arm where failure previously occurred. This was done in hopes of altering the point of failure. It was also thought that creating an arm with this 'X' shape would help to further reduce the occurring deflections by decreasing the deformation occurring in the vicinity of the mounting holes. Choosing the trajectory to take this shape allowed the arm to be symmetric and ideally universal.

4.1 Stage I – Simulations and Experiments

4.1.1 Original Unbraced Arm

The original unbraced arm was studied in two different commonly used control arm materials, 1020 Steel and 6061 Aluminum. This was done to draw a comparison between the mechanical characteristics of a steel arm versus those of an aluminum one. Both materials were studied using Pro-Engineer’s FEA module called Pro-Mechanica. Due to limitations in water jetting and CNC machine time and cost, the steel arm was not constructed and tested experimentally.

4.1.1.1 Steel

The first arm to be studied is the unbraced steel arm. This arm was studied using the techniques outlined in the methodology chapter of this paper. The same process was used for all of the arms in this study. The unbraced arm was modeled after a common control arm.

4.1.1.1.1 Stresses

The results of the FEA on the unbraced original arm using 1020 steel as the material showed stresses and deformation as expected. The steel arm developed stresses less than those observed in its 6061 aluminum counterpart. These results can be observed by comparing Figure 10 and Figure 13. The objective was to establish a basis for comparison between arms with no bracing and those with bracing. The aluminum arms with bracing were designed to evaluate whether or not they could produce results comparable to those of the steel arms.

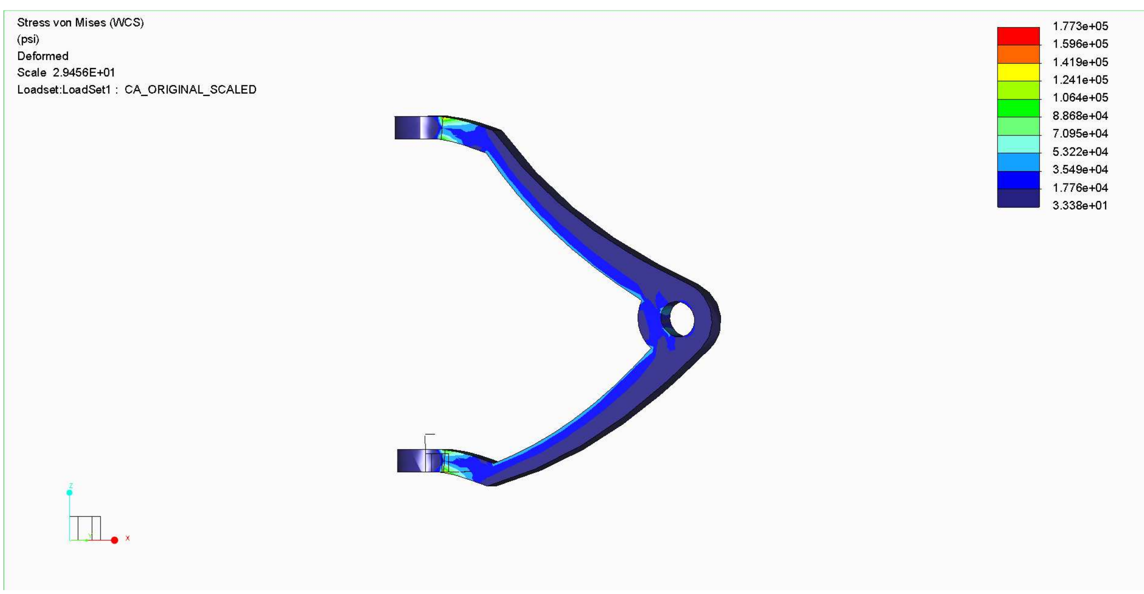

Figure 10 - Original Unbraced FEA Stress (1020)

The comparison between steel and aluminum arms is important because steel is the most commonly used control arm material. However, using aluminum as a substitute material in control arms is becoming more common in modern automobiles. This is because of aluminum’s many desirable mechanical properties and low relative cost. Previously, the advantages of aluminum did not outweigh the added cost of the material. Both of these specimens were tested through the use of an FEA with a load of 3500lbs.

4.1.1.1.2 Strains

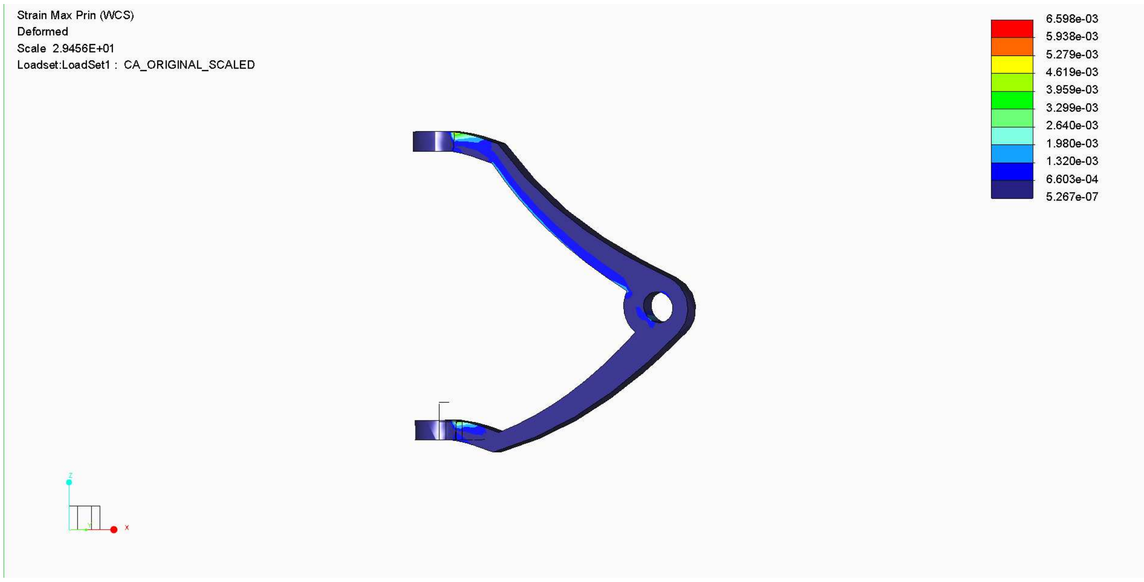

Figure 11 - Original Unbraced FEA Strain (1020)

The maximum principal strain for the unbraced steel arm as determined by the FEA was 6.598E-3 and that of the aluminum arm was determined to be 1.924E-2. Both of these results can be seen in Figures 11 and 14, respectively.

4.1.1.1.3 Deformation

Following the study of the maximum principal strains was the FEA study of the associated displacements for the same load of 3500lbs. Again as expected the steel arm was displaced less than the aluminum version. These results can be seen in Figures 12 and 15.

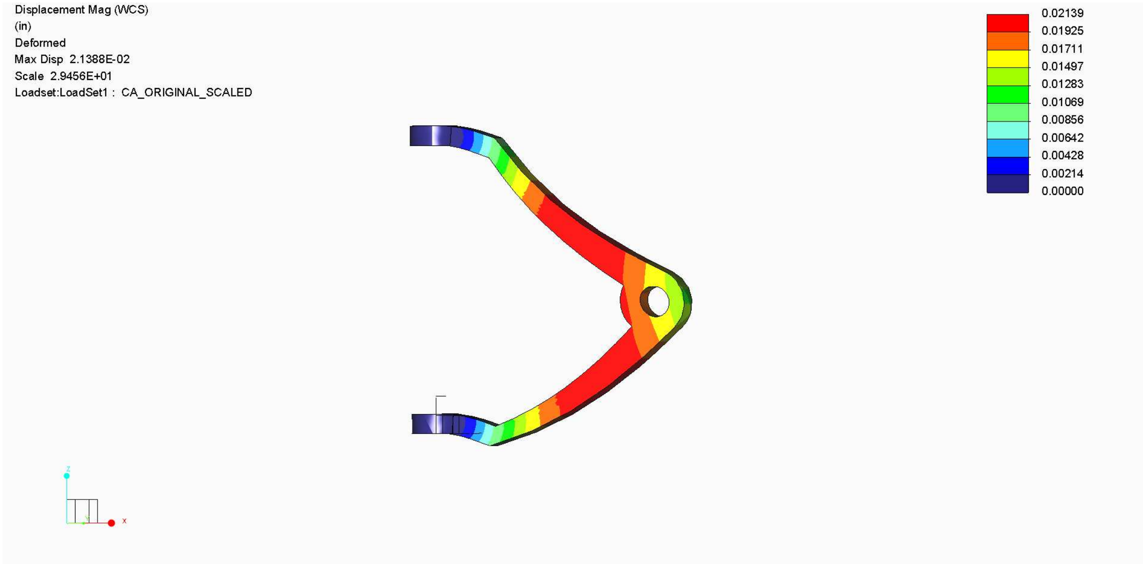

Figure 12 - Original Unbraced FEA Displacement (1020)

The unbraced steel arm during the FEA produced a displacement of 0.0214in while subjected to 3500lbs load. The load was kept constant for all specimens as defined by the constraints for the study. The Deformed option of the finite element analysis software was selected to help visualize how the experimental arms will deform under load. The 3500lbs testing load was determined experimentally. This was done by testing two sacrificial specimens. They were subjected to the same testing methods and procedures as the actual specimen were. This allowed us to determine a load where permanent deformation would occur. It was also performed to validate that the experimental procedure would perform as desired.

4.1.1.2 Aluminum

The same unbraced arm previously studied was re-analyzed for an aluminum alloy of 6061. The arm was studied following the standard procedure outlined previously. This was done to illustrate that an arm made of steel cannot be directly produced from aluminum and expected to perform on the same levels.

4.1.1.2.1 Stresses

The FEA of the unbraced aluminum arm showed heightened results in all categories when compared to its steel counterpart. Both the maximum von Mises stress and principal strains occurred at the location where the arm was constrained to the testing apparatus. This agrees with what was seen in the steel version of the same arm. Intuitively the results make sense since that portion of the arm is the location consisting of the least amount of material.

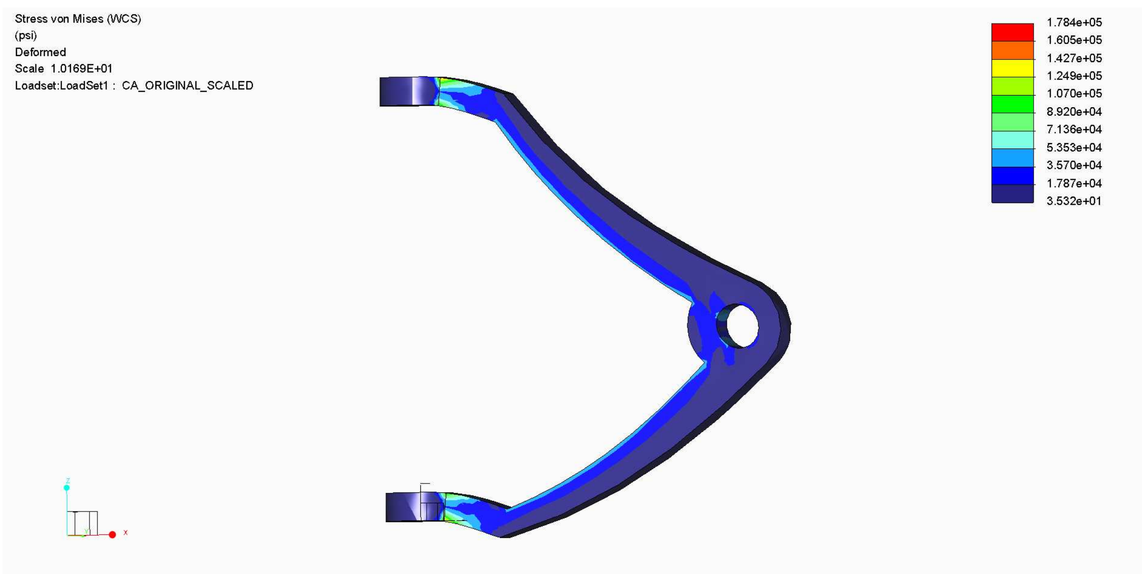

Figure 13 - Original Unbraced FEA Stress (Al 6061)

4.1.1.2.2 Strains

The maximum principal strains for the unbraced aluminum arm as determined from the FEA study can be seen in Figure 14. The maximum principal strain shown here is representative of the strain in the arm at its mounting location.

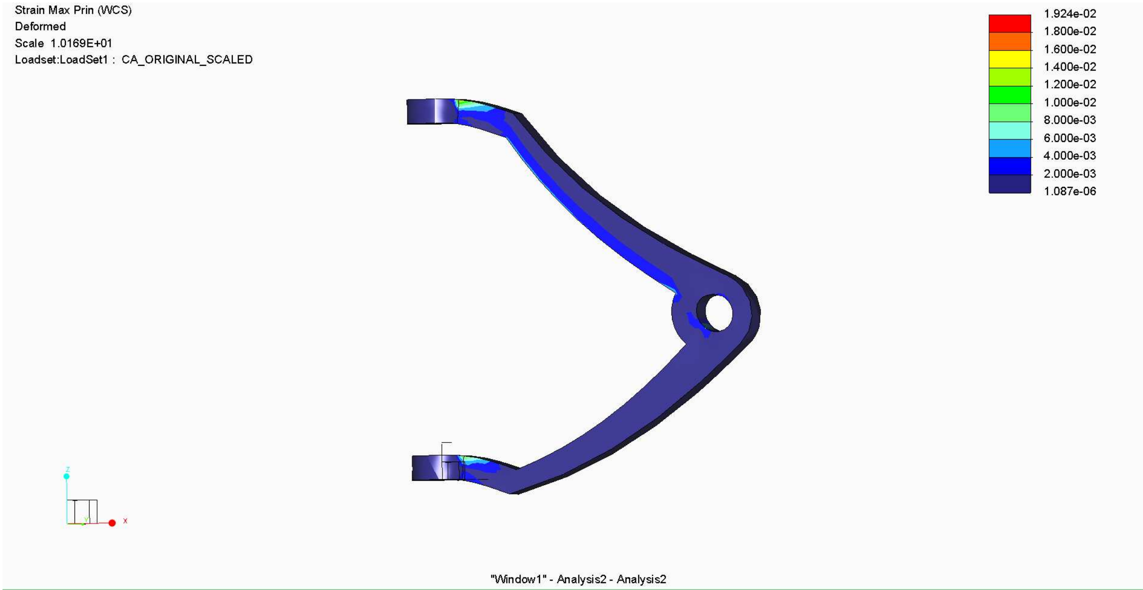

Figure 14 - Original Unbraced FEA Strain (Al 6061)

4.1.1.2.3 Deformations

The aluminum version of the unbraced arm deflected approximately 0.062in according to the finite element analysis as seen in Figure 15. This deflection is approximately three times as large as was seen in the steel version. When compared to the experimental results a significant difference in the deflections was detected. This is due to the way Pro-Engineer constrains the movement of the arm. The FEA study constrains the entire inner surface of the mounting holes and does not account for the elongation of the mounting features. During the physical experiment it was noted that the holes became slightly deformed and elongated into a more oval shape. This elongation is believed to have introduced some additional deflection in the test specimen.

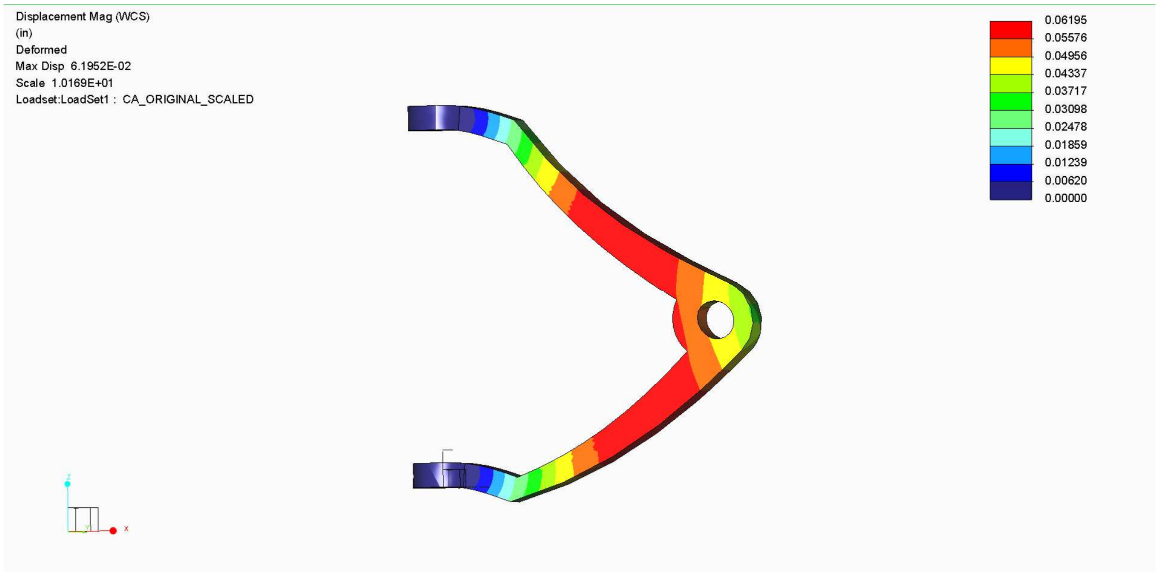

Figure 15 - Original Unbraced FEA Displacement (Al 6061)

The experimental defection and associated loads can be seen in Figure 16. At a load of approximately 3500lbs the unbraced arm deflected 0.14in. This is approximately twice the value calculated in FEA simulation; this is due to the experimental error and the inconsistencies between how the deformation is simulated using ideal conditions and the manner in which it actually deforms in experiments.

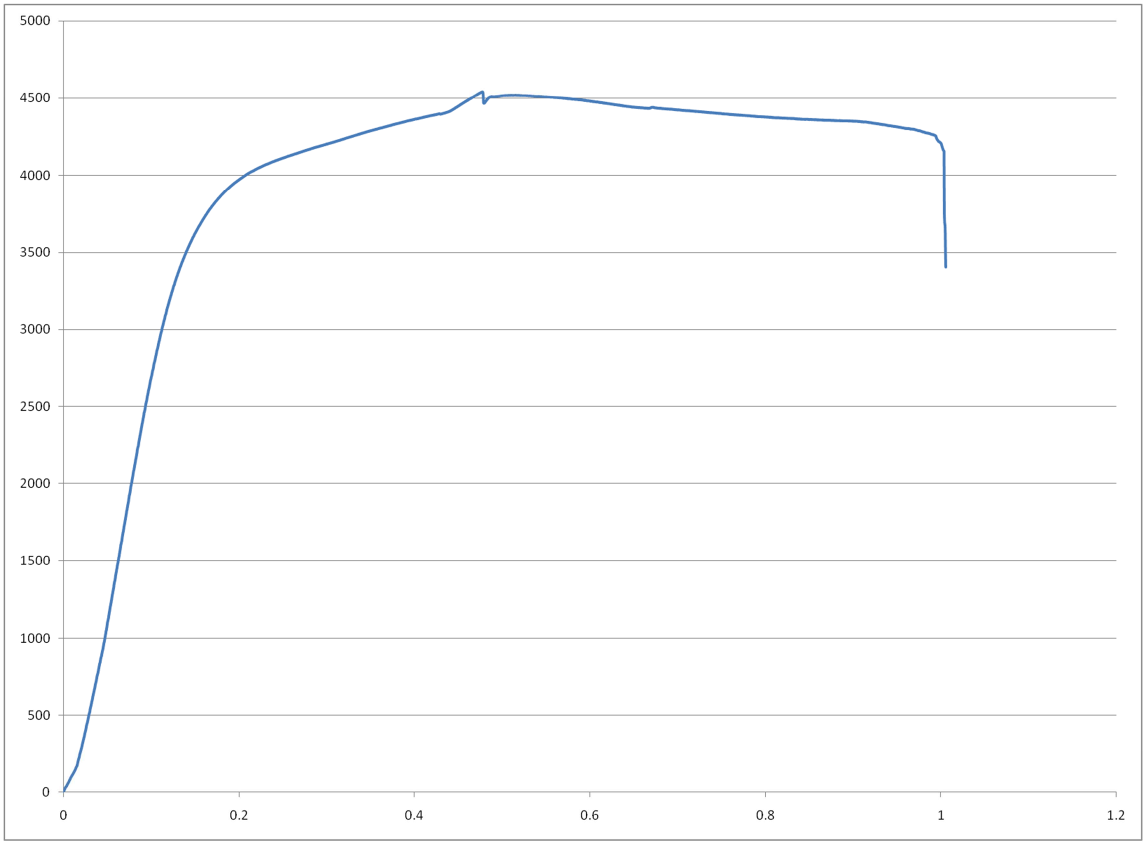

Figure 16 - Original Load vs. Deflection Graph

The graphed data from physical testing of the unbraced arm produced acceptable results. It can be seen in Figure 16 that the unbraced arm deflected to approximately 1in before fracturing. The arm also reached a peak load of approximately 4500lbs. The peak load for this arm is comparable to the peak load required to fracture the braced arms following the 'Z' shaped trajectory. This indicates that the addition of bracing in this trajectory has little impact on the ultimate strength of the specimen; however, it became evident that the bracing did significantly lessen the amount of deflection that occurred in each of the specimen regardless of the cross sectional shape used.

4.1.2 Webbed Arm – Square Cross Section

The following arms throughout the remainder of the study will be utilizing bracing members on the interior of the control arm. The first cross sectional shape studied was a square. The square shape used here had dimensions of 0.223” x 0.223”. The square followed the same ‘Z’ trajectory as all of the arms studied in Stage I of this study.

4.1.2.1 Stresses

To assess the effects of adding bracing members to the interior section of a control arm on deflections, a square cross section shape was first used and followed a standard ‘Z’ trajectory. The dimensions of the square were manipulated to be equivalent to a cross sectional area of 0.05 in^2. This area was held constant for all shaped used throughout the remainder of this study.

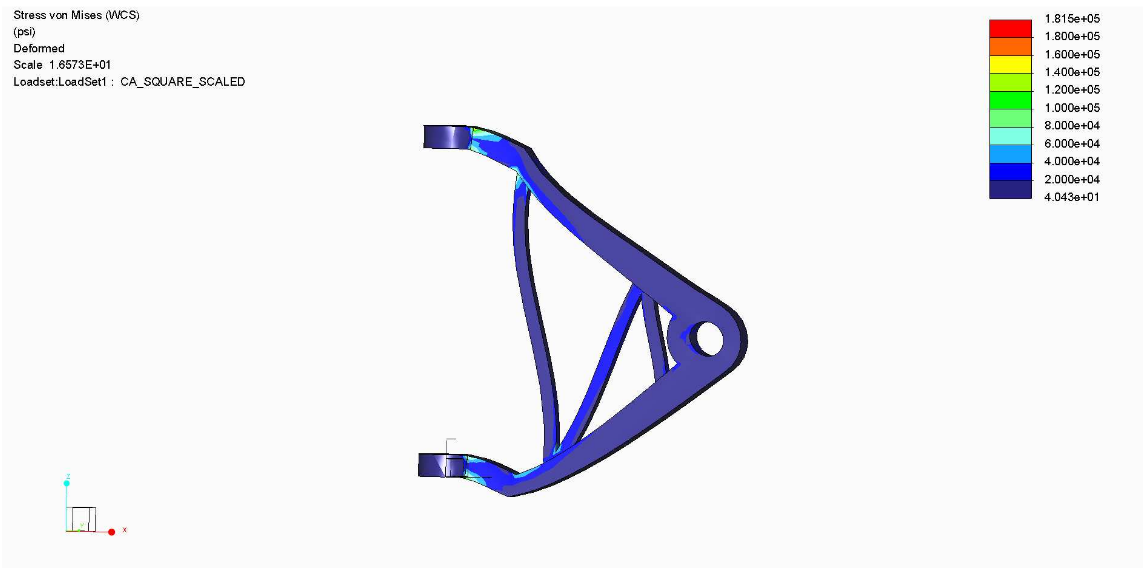

Figure 17 - Square FEA Stress

Figure 17 shows the results obtained in the stress analysis of the square shaped bracing members. The results show that the maximum von Mises stress that occurred was increased from that of the unbraced arm. However, that stress was more localized at the mounting locations and decreased in the outer element of the arm. It can also be seen that the center member of the cross bracing experienced a heightened stress level as did some of the points where the bracing merged with the arms outer elements.

4.1.2.2 Strains

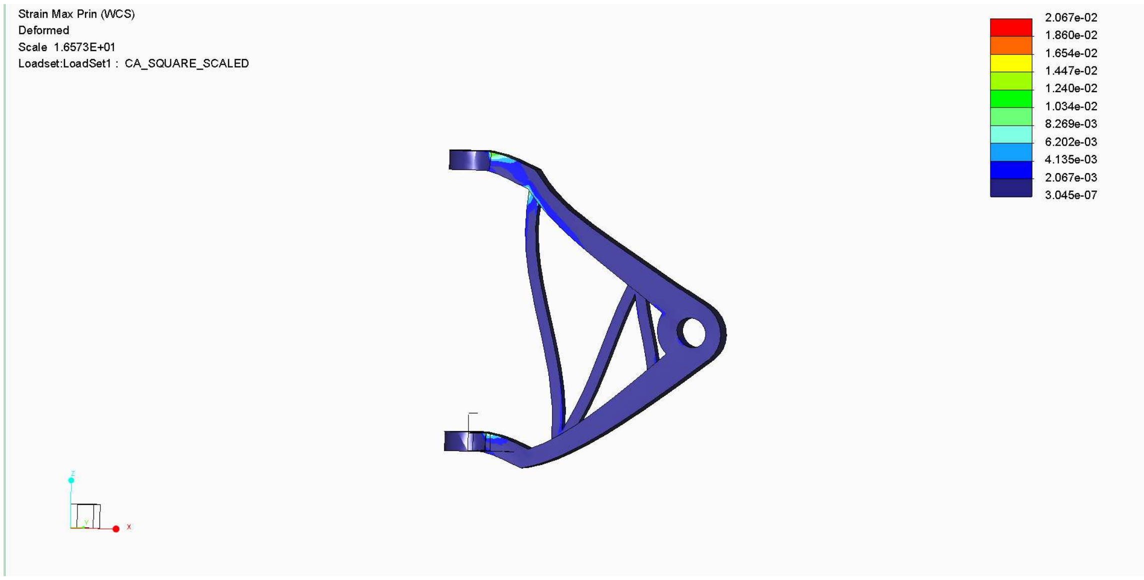

Figure 18 - Square FEA Strain

The strain analysis showed similar results to those of the stress analysis. The strain at the mounting locations was increased and more concentrated. It also showed that the bracing members were being strained as well; these results can be observed in Figure 18. Similarly, as seen in the stress analysis, the outer members of the arms were relieved of some of the strains they had experienced before the addition of the cross bracing.

The displacement of this arm was studied also using the FEA capabilities of Pro-Engineer. The results of the displacement study can be observed in Figure 19. The results show that all though there were increases in both the stress and strain at particular points there was a decrease in the deflections that occurred in the arm. Under the 3500lb load the braced arm showed a maximum displacement of 0.038 in, a reduction in deflection of approximately 40% when compared to the unbraced arm of the same material. However, it still managed to deflect more than the unbraced 1020 steel control arm.

4.1.2.3 Deformations

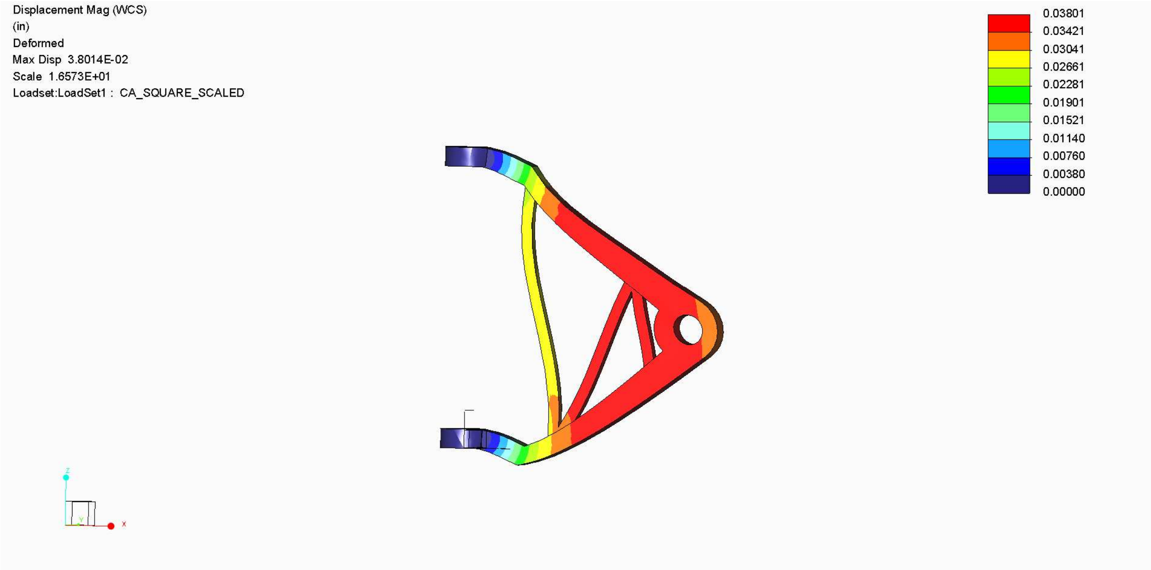

Figure 19 - Square FEA Displacement

In addition to the FEA studies the square arm was also manufactured and tested physically. The arm was tested following the same procedure outlined in the previous experimental tests. As observed in the unbraced arm, the maximum deflection when subjected to a 3500 lbs. load did not agree with the FEA study. This is believed to be for the same reasons as were mentioned before. The FEA study showed a maximum deflection of approximately 0.038 in while the experiments produced deflections in the range of 0.07 in. The graphed results from experimental test are shown in Figure 20. The difference in these results is similar to the differences noticed in the results of the unbraced arm.

The square arm managed to produce a relatively smooth load vs. deflection curve. The curve shows that the arm failed quite suddenly. The peak load the square arm was able to with stand was approximately 4400lbs. This peak load is respectably close to that of the unbraced arm; however, the deflection in this arm proved to be significantly less.

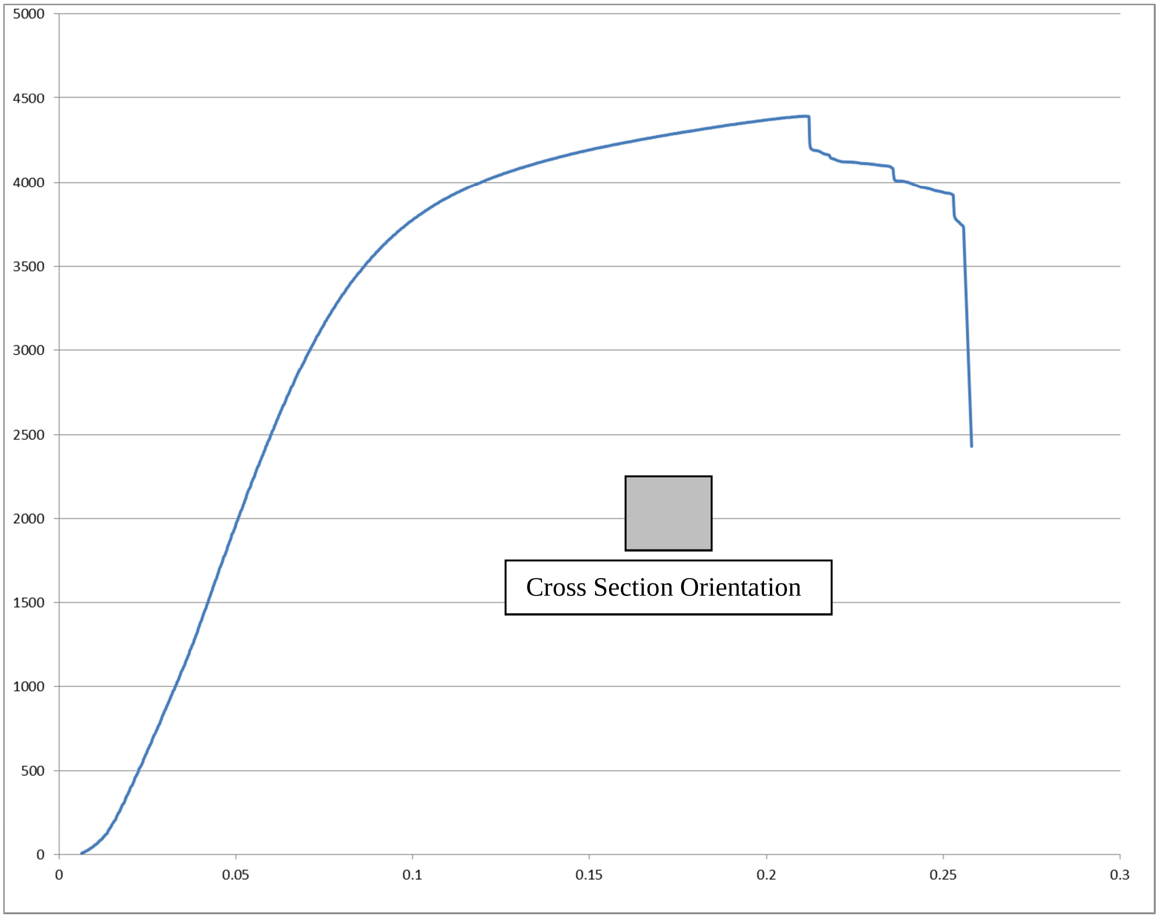

Figure 20- Square Load vs. Deflection Graph

4.1.3 Webbed Arm - Rectangle I Cross Section

In order to continue evaluating the effects that the addition of bracing members has on deflections occurring in a control arm, a rectangular shape was also tested. The rectangular cross section followed the same standard ‘Z’ trajectory as previously used. The dimensions of the rectangle were again manipulated to be equivalent to a cross sectional area of 0.05 in^2. The dimensions of the rectangular cross section were 0.158” x 0.316”. This same rectangular shape was studied in two different orientations; the second orientation will be discussed in the following section.

4.1.3.1 Stresses

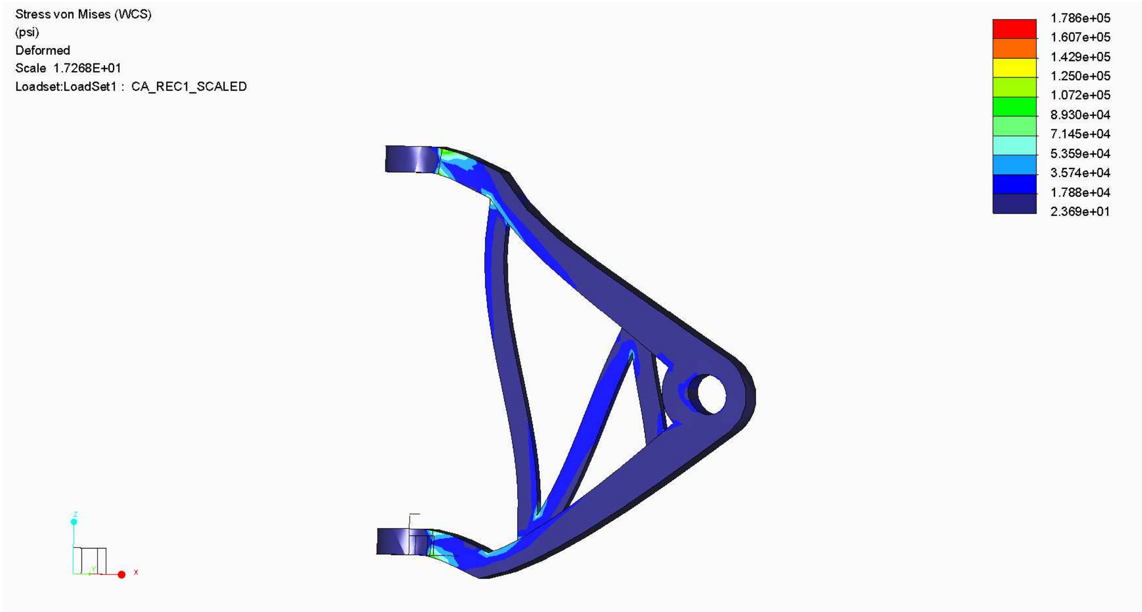

Figure 21 - Rectangle I FEA Stress

Similar, to the square arm the first step in evaluating the effectiveness of a cross bracing utilizing a rectangular cross sectional shape was to perform an FEA study. The study was performed in the same manner as used in the previous arms configurations. Figure 21 shows the results obtained in the stress analysis of the arm with rectangular shaped bracing members. The results show that the maximum von Mises stress that occurred increased from that of the unbraced arm. Although once again, the stress showed to be more concentrated at the mounting locations and decreased in the outer elements of the arm. It can also be seen that the center member of the cross bracing experienced a heightened stress level as did some of the points where the bracing merged with the arms outer elements. These results were comparable to those of the arm utilizing the square shaped bracing.

4.1.3.2 Strains

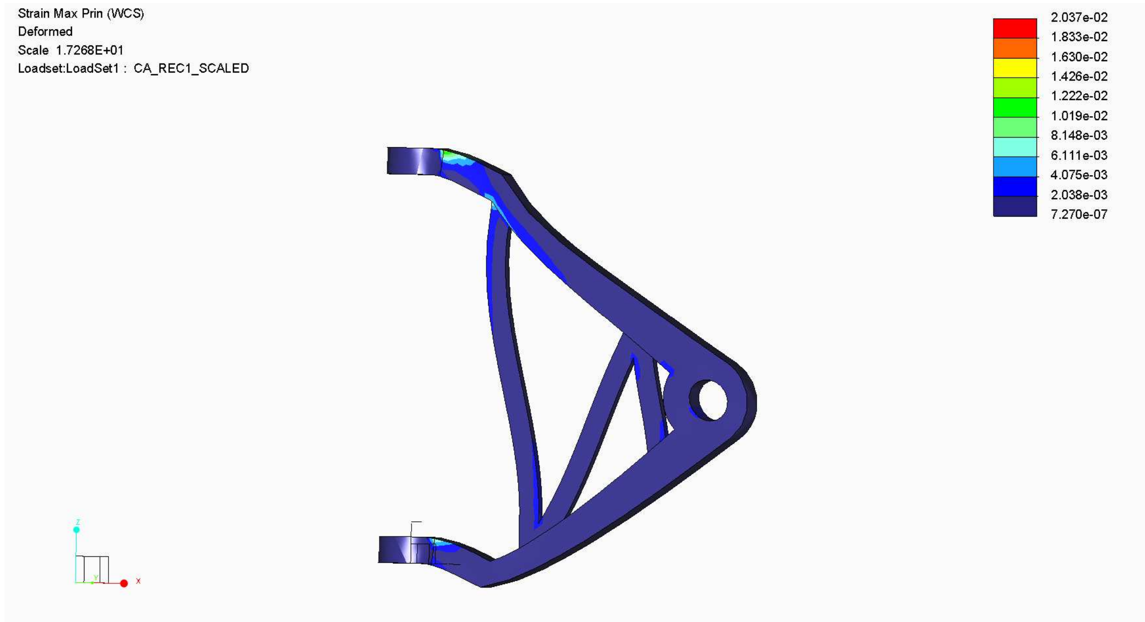

Figure 22 - Rectangle I FEA Strain

Following the stress analysis was the FEA maximum principal strain study. The strain analysis showed similar results to those of the stress analysis. The strain at the mounting locations was increased and more concentrated. It also showed that the bracing members became strained as well; these results can be observed in Figure 22. These results are comparable to those found in the square maximum principal strain analysis, the outer members of the arms were relieved of some of the strains they had experienced before the addition of the cross bracing.

4.1.3.3 Deformations

The displacement produced by this arm was also studied using the FEA capabilities of Pro-Engineer. The results of the displacement study can be observed in Figure 23. The results show increases in both the stresses and strains at particular points as well as a decrease in the deflection of the arm. Under the 3500lb load, the rectangle I arm produced a maximum displacement of 0.0365 in. That is a reduction in deflection, by an even larger percentage than was observed in the square arm, when using the same material.

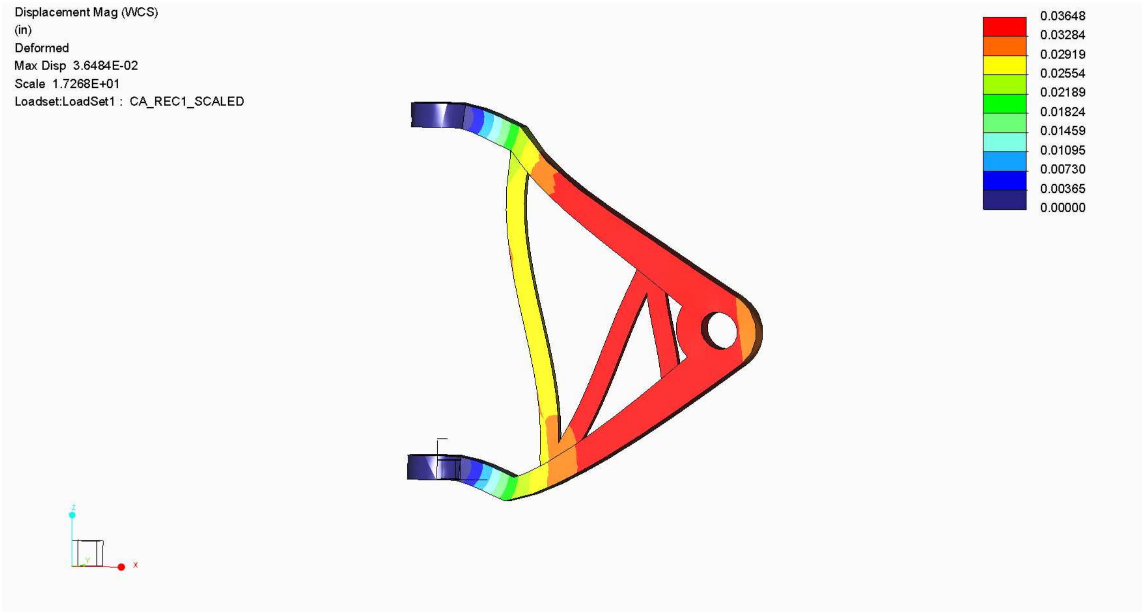

Figure 23 - Rectangle I FEA Displacement

The maximum deflection that occurred was greater than the deflection of the unbraced steel arm but less than the deflection of the unbraced aluminum arm. In addition to the FEA studies, the rectangle I arm, was also manufactured and tested experimentally. The arm was tested following the same procedure outlined in the previous experimental tests. As observed in the previous studies, the maximum deflection when subjected to a 3500 lbs. load did not agree with the FEA study. This is again for the same reasons as were mentioned before. The FEA study showed a maximum deflection of approximately 0.0365 in while the experimental results showed deflections in the range of 0.075 in. The graphed results from the experimental test can be viewed in Figure 24. The difference in these results is similar to the differences noticed in the results of the previous arms.

The rectangle I arm managed to produce a relatively jagged load vs. deflection curve. The curve shows that the arm failed quite suddenly as was seen with the square arm. The peak load the rectangle I arm was able to with stand was approximately 4500lbs. This peak load is also respectably close to that of the unbraced arm; however, the deflections in this arm proved to be significantly less.

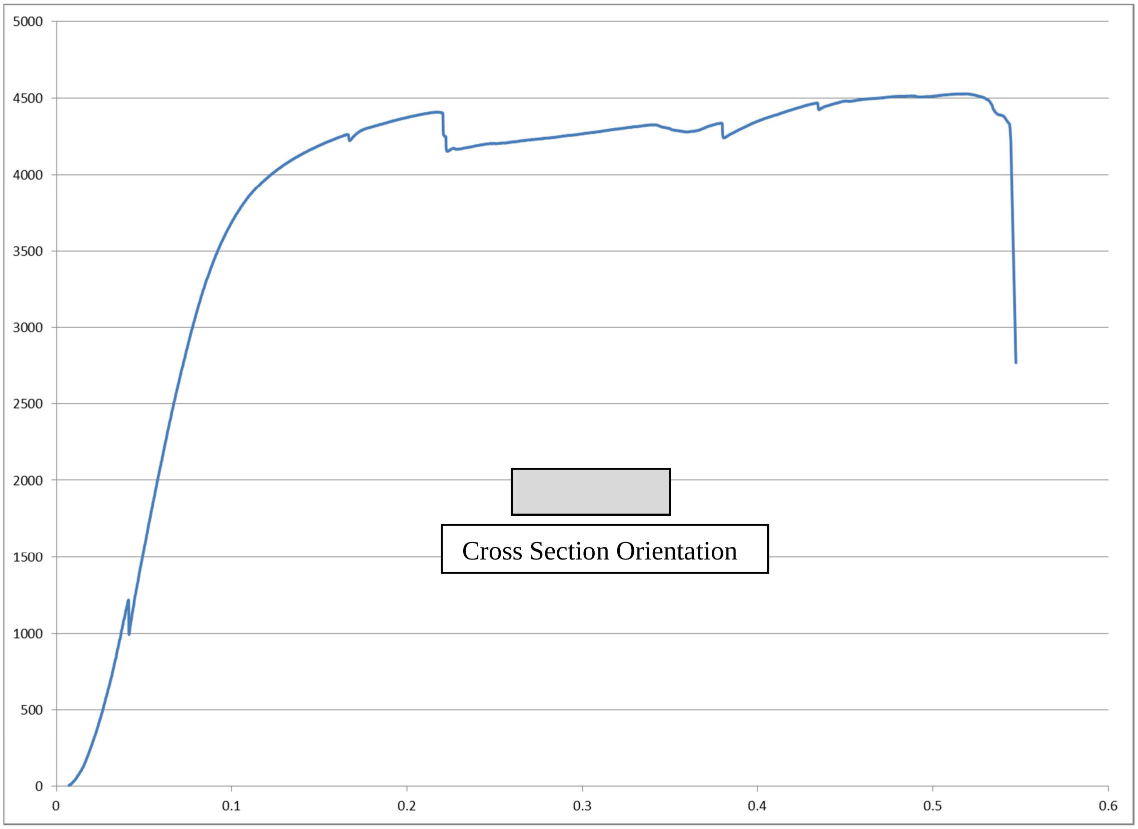

Figure 24 - Rectangle I Load vs. Deflection Graph

4.1.4 Webbed Arm - Rectangle II Cross Section

Next, to continue evaluating the effects that the addition of bracing members has on deflections occurring in a control arm, a second rectangular shape was also tested. The rectangular cross section was the same as used in the previous study and followed the same standard ‘Z’ trajectory. The dimensions of the rectangle were again manipulated to be equivalent to a cross sectional area of 0.05 in^2. This same rectangular shape was rotated 90 degrees from the previous study, to determine if the orientation of the shape will affect the associated deflections in the control arm.

4.1.4.1 Stresses

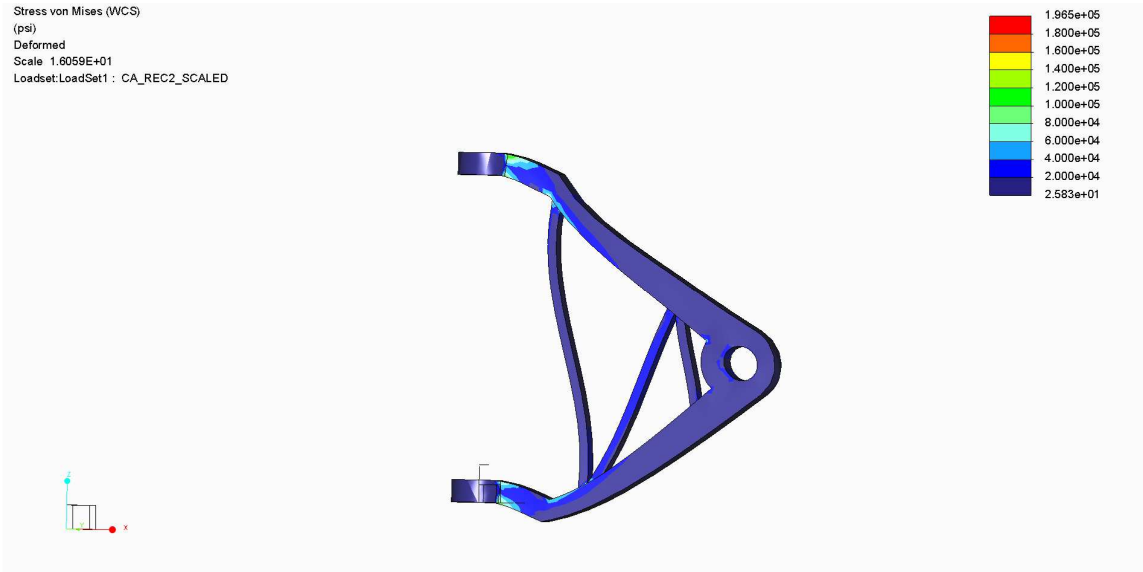

Figure 25 - Rectangle II FEA Stress

Following the same approach used for the previous arms the first step in evaluating the effectiveness of a cross bracing utilizing a rectangular II cross sectional shape was to perform an FEA study. The study was performed in the identical manner as used in the previous arm configurations. Figure 25 shows the results obtained in the stress analysis of the arm with rectangular II shaped bracing members. The results show that the maximum von Mises stress that occurred again increased from that of the unbraced arm. On the contrary, the stress was more concentrated at the mounting locations and decreased in the outer elements of the arm. It can also be seen that the center member of the cross bracing experienced a heightened stress level as did some of the points where the bracing merged with the arms outer elements. These results are comparable to those of the previous arms utilizing the inner bracing members.

4.1.4.2 Strain

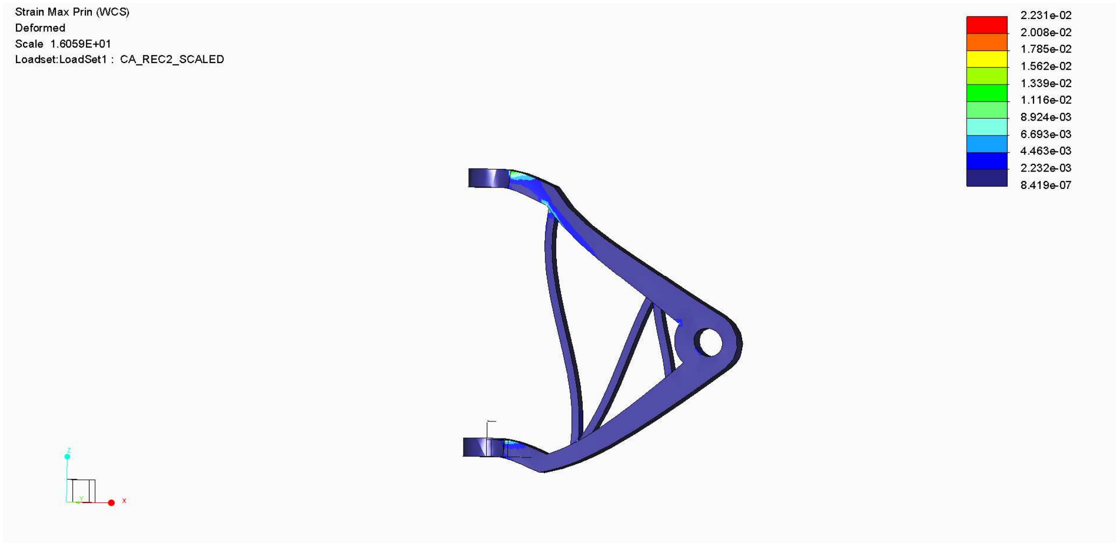

Figure 26 - Rectangle II FEA Strain

The previous stress analysis was then preceded by a FEA of the maximum principal strain. The strain analysis showed similar results to those of the stress analysis. The strain at the mounting locations was increased and more concentrated. It also showed that the bracing members became strained as well; these results can be observed in Figure 26. These results are comparable to those found in the previous maximum principal strain analyses, the outer members of the arms were relieved of some of the strains they had experienced before the addition of the cross bracing.

4.1.4.3 Deformations

Following the strain study, the displacement produced by this arm was also evaluated using the FEA capabilities of Pro-Engineer. The results of the displacement study can be observed in Figure 27. The results agree with those of the previous studies. Under the 3500lb load, the rectangle II arm produced a maximum displacement of 0.039in which is an increase in deflection when compared to the previous braced arm studies. However, compared to the unbraced arm, the deflections were still significantly decreased for the same material.

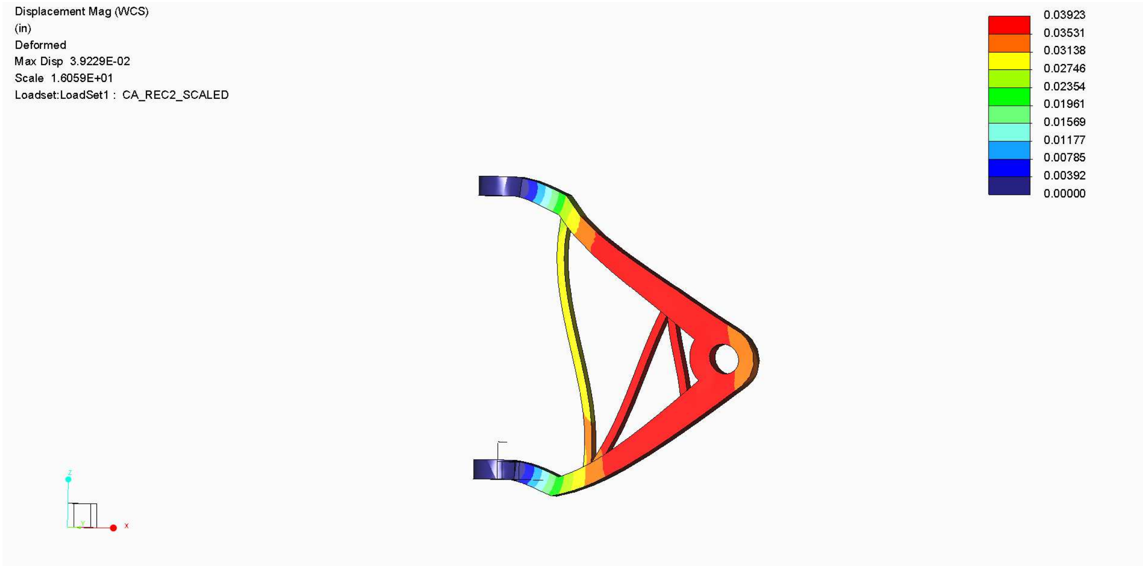

Figure 27 - Rectangle II FEA Displacement

The maximum deflection that occurred was greater than that produced by the unbraced steel arm; however, it was less than that of the unbraced aluminum arm. In addition to the FEA studies, the rectangle II arm, was also manufactured and tested physically. The arms were tested following the same procedure outlined in the previous experimental tests. This particular arm was tested twice; two identical specimens for this arm were produced and tested to ensure the results/data was repeatable. The results from the two samples yielded comparable results and nearly identical load vs. deflection curves. As was observed in the previous studies, the maximum deflection when subjected to a 3500 lbs. load did not agree with the FEA study. This is believed to be for the same reasons as were previously mentioned. The FEA study showed a maximum deflection of approximately 0.039in while the experimental results produced deflections of approximately 0.135in. The graphed results from the experimental test can be see in Figure 28. The difference in these results is greater than the differences noticed in the results of the previous arms.

The rectangle II arm managed to produce a relatively smooth load vs. deflection curve. The curve depicts that the arm failed suddenly as was seen with the previous arms. The peak load with which the rectangle II arm was able to with stand shows to be approximately 4600lbs. This peak load is close to that of the previous arms; however, it was able to with stand a load of approximately 100lbs more than the previous rectangle orientation. Despite the fact that this arm with stood a greater load than the previously studied braced arms it actually deflected nearly the same as the unbraced aluminum arm.

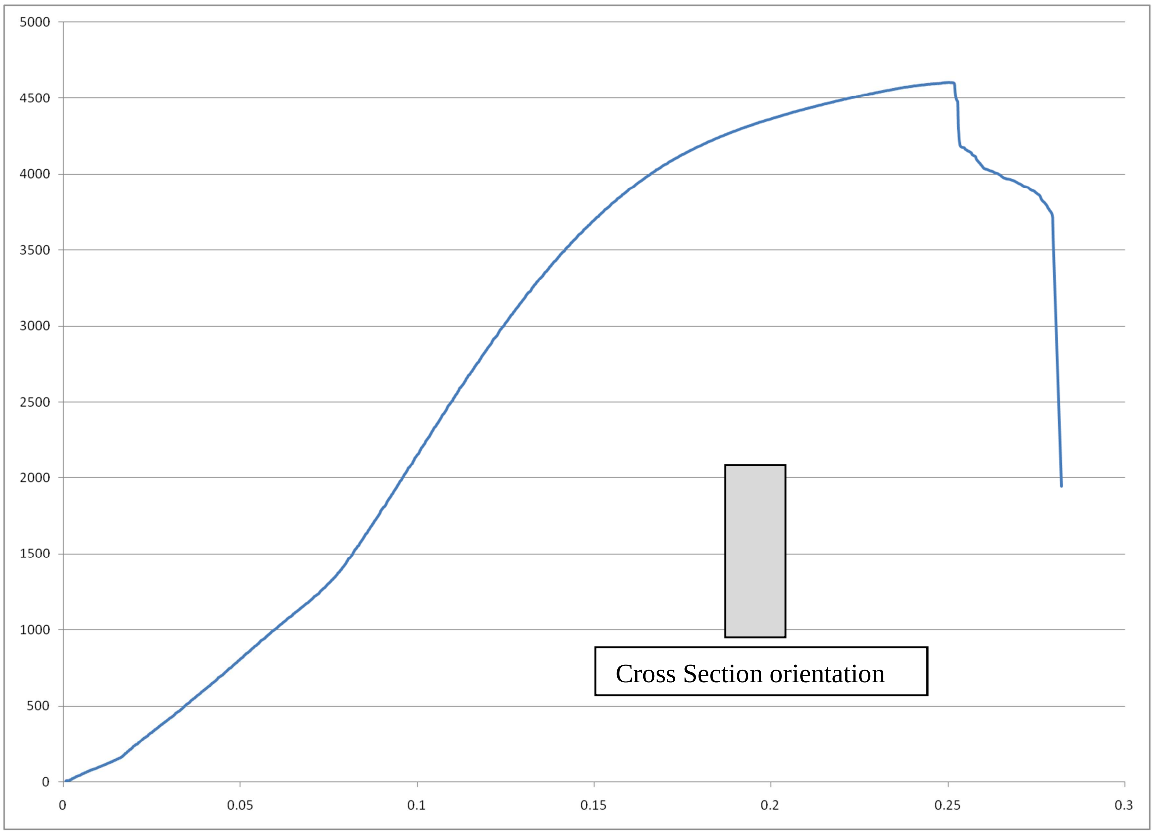

Figure 28 - Rectangle II Load vs. Deflection Graph

4.1.5 Other Web Cross Sectional Shapes

In addition, other control arm configurations were studied as well. The following arms were evaluated using the finite element capabilities of Pro-Engineer only. Initially the preceding arms were planned to be studied by a physical experiment as well;

however, during the manufacturing stage the shapes were deemed too difficult to manufacture consistently. This was due to limitations in available machinery and programming. Additionally, the arms would be difficult to for an industry to produce on a large scale. Therefore it was determined they would be studied using the FEA capabilities only, simply shapes are basic common shapes.

4.1.5.1 Triangular Cross Sectional Web

The first arm of the additional shapes studied, to continue evaluating the effects that the addition of bracing members has on deflections occurring in a control arm, was a triangular shape. The triangular cross section was oriented in a way such that the base of the triangle was coplanar with the surface of the arm. The trajectory of the triangular bracing followed the same standard ‘Z’ shape as the previously studied arrangements. The dimensions of the triangle were manipulated to be equivalent to a cross sectional area of 0.05 in^2. The triangle used was an equilateral triangle in order to keep the shape symmetric. The triangular cross section was composed of an equilateral 60 degree triangle with sides of length 0.339 in.

4.1.5.1.1 Stresses

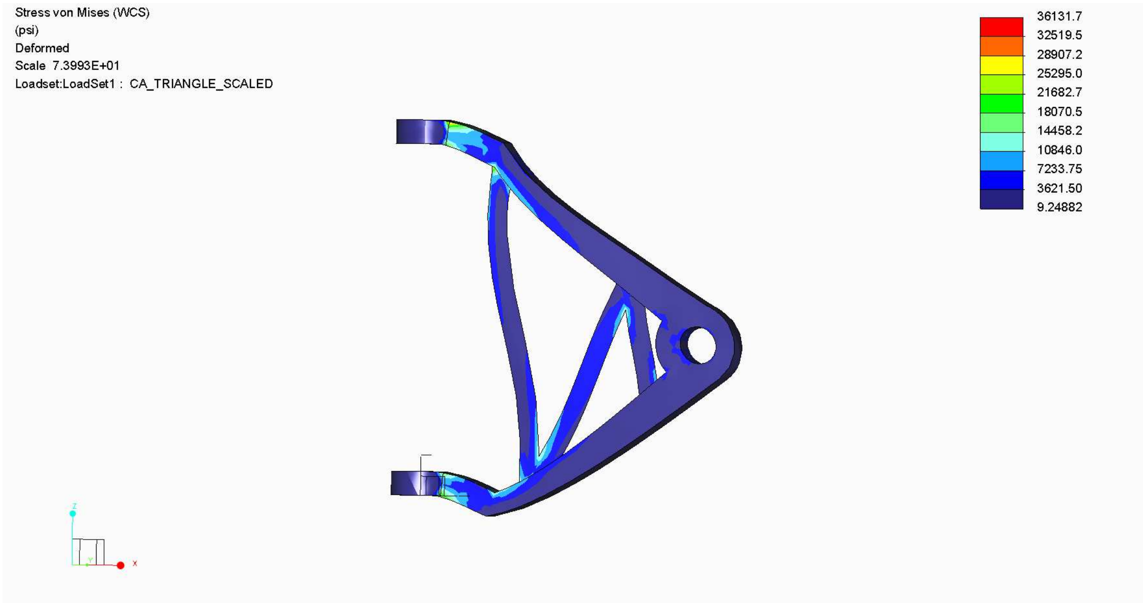

Figure 29 - Triangle FEA Stress

Following the same approach used for the previous arms, the first step in evaluating the effectiveness of a cross bracing utilizing a triangular cross sectional shape was to perform an FEA study. The study was performed in the identical manner as was used in the previous arm configurations. Figure 29 shows the results obtained in the stress analysis of the arm with triangular shaped bracing members. The results show that the maximum von Mises stress that occurred again increased from that of the unbraced arm. The stress is seen to be more concentrated at the mounting locations and smaller in the outer elements of the arm. It can also be seen that the center member of the cross bracing experienced a heightened stress level as did some of the points where the bracing merged with the arms outer elements. These results are comparable to those of the previous arms utilizing the inner bracing members. It can be seen that the general trend is that the addition of bracing relocates a portion of the stress to a particular location in each arm tested thus far. It can be seen, that the addition of bracing members does change the way in which a control arm distributes applied loads.

4.1.5.1.2 Strains

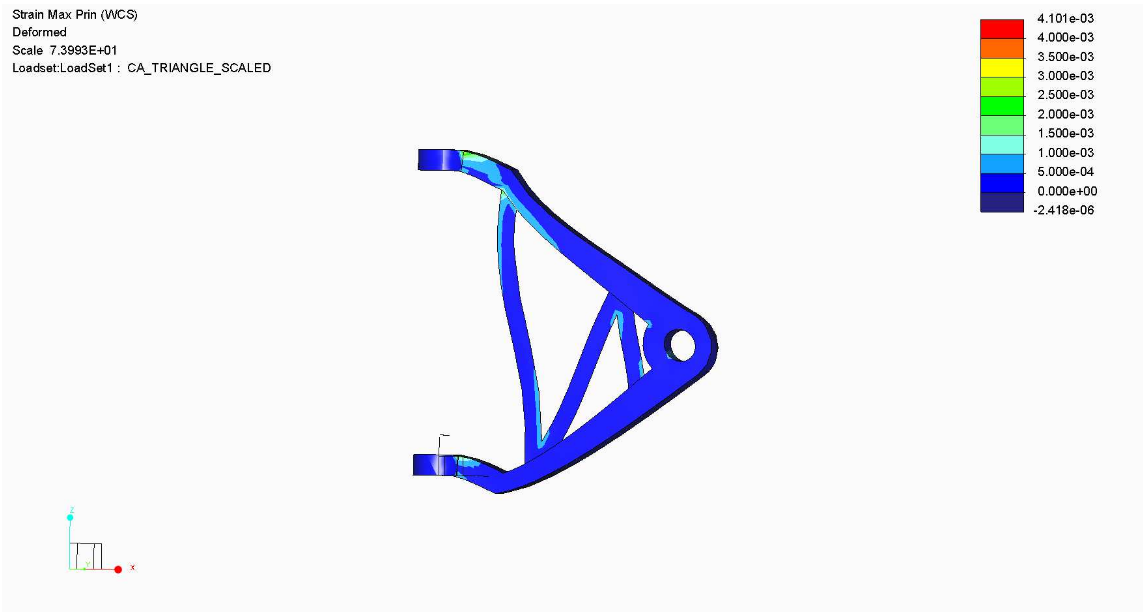

Figure 30 - Triangle FEA Strain

The previous stress analysis was then preceded by a FEA of the maximum principal strain. The strain analysis showed similar results to those of the stress analysis. The strain at the mounting locations was increased and more concentrated. It also showed that the bracing members became strained as well; these results can be observed in Figure 30. The results are comparable to those found in the previous maximum principal strain analyses. The outer members of the arms were relieved of some of the strains they had experienced before the addition of the cross bracing.

4.1.5.1.3 Deformations

Following the strain study, the displacement produced by this arm was also evaluated using the FEA capabilities of Pro-Engineer. The results of the displacement study can be observed in Figure 31. The results agree with those of the previous studies, although there were increases in both the stresses and strains at particular points there was a general decrease in the deflections that occurred in the arm. Under the 3500lb load, the triangular arm produced a maximum displacement of 0.0085 in. This is a decrease in deflection when compared to any of the previous braced arm studies. Furthermore, the triangular shaped bracing deflected less than both the steel and aluminum unbraced arms. This is due to the geometry of the triangle and the way in which it deforms.

Due to limitations in the available machining equipment the triangular arm was not tested physically. Though it is believed, this arm would have produced results following the general pattern between the FEA and the actual experiment. If the addition of bracing members is to be incorporated in to common control arms, the triangular cross section should be further considered. This is of course with the understanding of the difficulties associated in the manufacturing process.

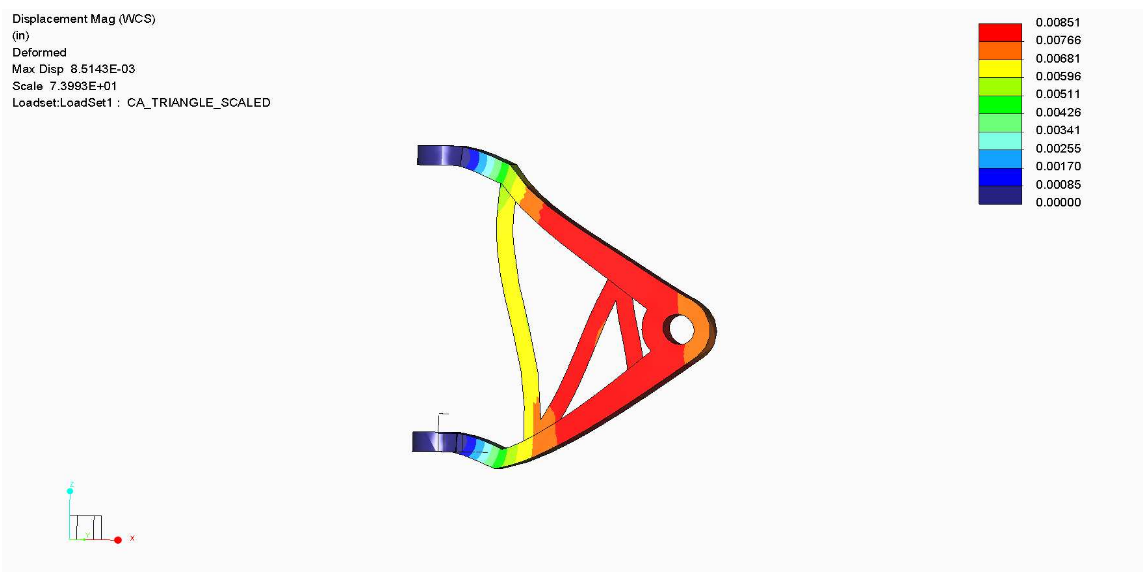

Figure 31 - Triangle FEA Displacement

4.1.5.2 Circular Cross Sectional Web

The second arm of the additional shapes studied, to continue evaluating the effects that bracing members have on deflections occurring in control arms, was a circular shape. The trajectory of the circular bracing followed the same standard ‘Z’ shape as the previously studied arrangements. The circular cross section used had a diameter of 0.2523” and produced a cross sectional area of 0.05 in^2.

4.1.5.2.1 Stresses

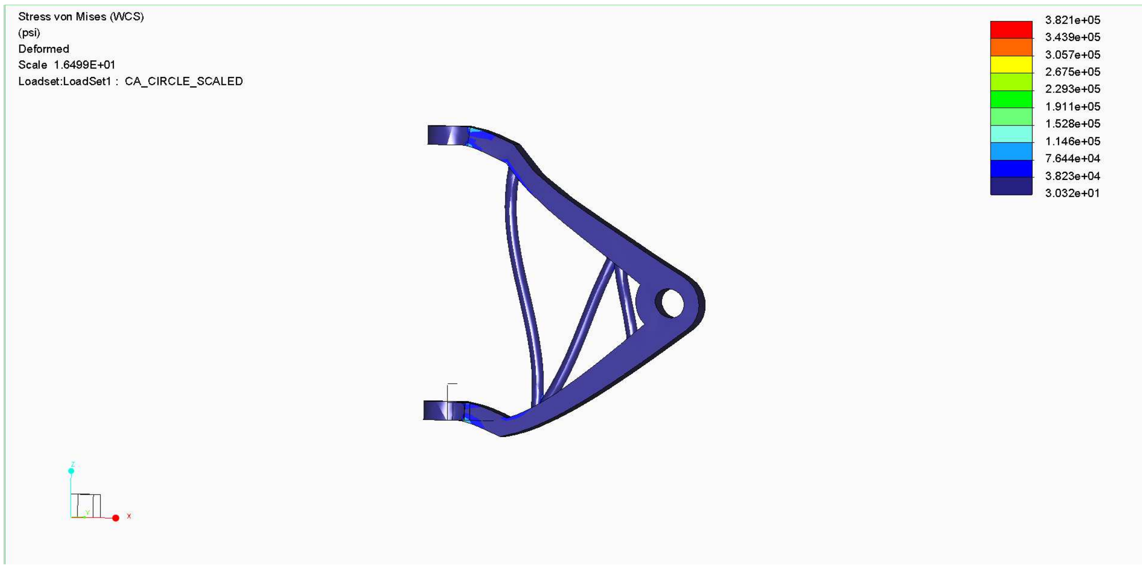

Figure 32 - Circle FEA Stress

Following the same approach used for the previous arms, the first step in evaluating the effectiveness of a cross bracing utilizing a circular cross sectional shape was to perform an FEA study. The study was performed in the identical manner as was used in the previous arm configurations. Figure 32 shows the results obtained in the stress analysis of the arm with circular shaped bracing members. The results show that the maximum von Mises stress that occurred again increased from that of the unbraced arm. On the contrary, the stress showed to be more concentrated at the mounting locations and decreased in the outer elements of the arm. It can also be seen that the center member of the cross bracing experienced a heightened stress level as did some of the points where the bracing merged with the arms outer elements. These results are comparable to those of the previous arms utilizing the inner bracing members. It can be seen that this arm as well follows the general trend in that the addition of bracing relocates a portion of the stress to a particular location in each arm. It can be seen, that the addition of bracing members changes the way in which a control arm distributes applied loads.

4.1.5.2.2 Strains

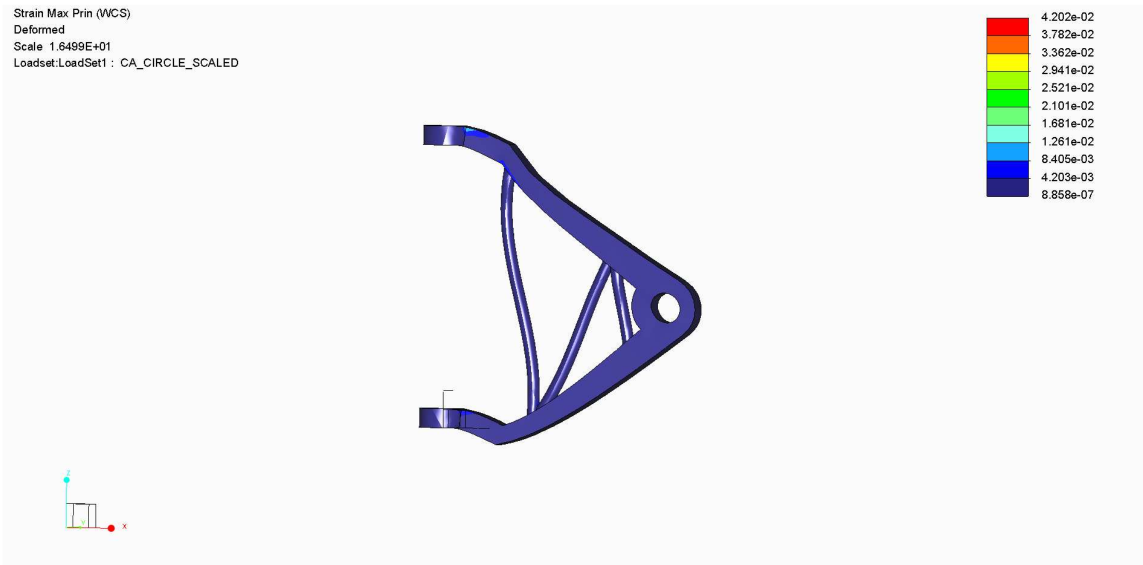

Figure 33 - Circle FEA Strain

The previous stress analysis was then preceded by a FEA of the maximum principal strain. The strain analysis showed similar results to those of the stress analysis. The strain at the mounting locations was increased and more concentrated. It also showed that the bracing members became strained as well; these results can be observed in Figure 33. The results are comparable to those found in the previous maximum principal strain analyses. The outer members of the arms were relieved of some of the strains they had experienced before the addition of the cross bracing.

4.1.5.2.3 Deformations

Following the strain study, the displacement produced by this arm was also evaluated using the FEA capabilities of Pro-Engineer. The results of the displacement study can be observed in Figure 34. The results agree with those of the previous studies, although there were increases in both the stresses and strains at particular points there was a decrease in the deflections that occurred in the arm. Under the 3500lb load, the circular arm produced a maximum displacement of 0.0382 in. That is a decrease in deflection when compared to unbraced aluminum arm. However, the circular shaped bracing managed to deflect comparably to the other braced arms.

Due to limitations in the available machining equipment the circular arm was not tested physically. Though it is believed, this arm would have produced results following the general pattern between the FEA and the actual experiment. If the addition of bracing members is to be incorporated in to common control arms, the circular cross section should be further considered. This is of course with the understanding of the difficulties associated with the manufacturing process.

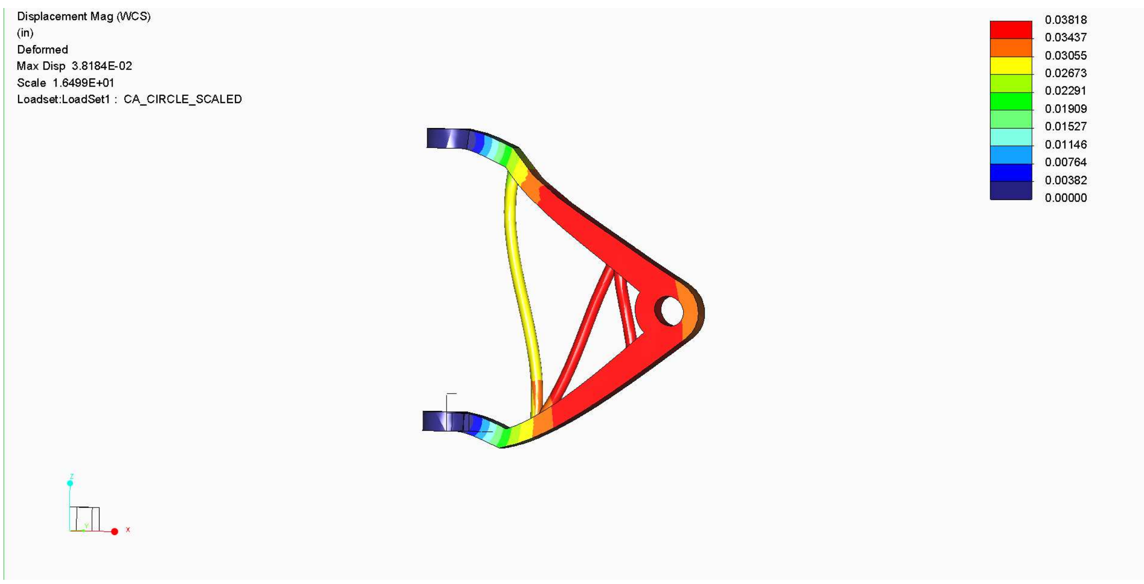

Figure 34 - Circle FEA Displacement

4.2 Stage II – Simulations and Experiments

4.2.1 Webbed Arm - Rectangle I Cross Section

To begin further studying the effects of bracing on control arms the same cross sectional shapes were used as in stage I. The shapes now followed the new 'X' shaped trajectory. To begin stage II the rectangular I shape was selected to be studied by both FEA and experimentally. This was done in order to validate the results obtained by the FEA. Two specimen of the rectangle I shape following the 'X' trajectory were produced. The purpose of creating two of these samples was to ensure that the data and results obtained were repeatable. This is similar as to what was done in with rectangle II in stage I of this study. The remaining shapes will be evaluated using the finite element capabilities of Pro-Engineer.

4.2.1.1 Stresses

The first step in evaluating the effectiveness of the 'X' trajectory bracing utilizing a rectangle I cross sectional shape was to perform an FEA study. The study was performed in the same manner as was used in the previous shapes and arms of stage I. The cross sectional areas were again held constant at $0.05in^2$. Figure 35 shows the results obtained in the stress analysis of the rectangle I shaped bracing members. The results show that the maximum von Mises stress that occurred was decreased from that of the unbraced arm. While studying the 'Z' shaped trajectory it was observed that there was an increase in the maximum von Mises stress. It can also be seen that now both of the center members of the cross bracing are experiencing stress. Similarly, to the previous rectangle I shape and 'Z' trajectory the bracing members are redistributing the applied load. However, in the 'X' configuration the bracing members appear to be evenly taking on portions of the stress that once occurred in the arms outer elements.

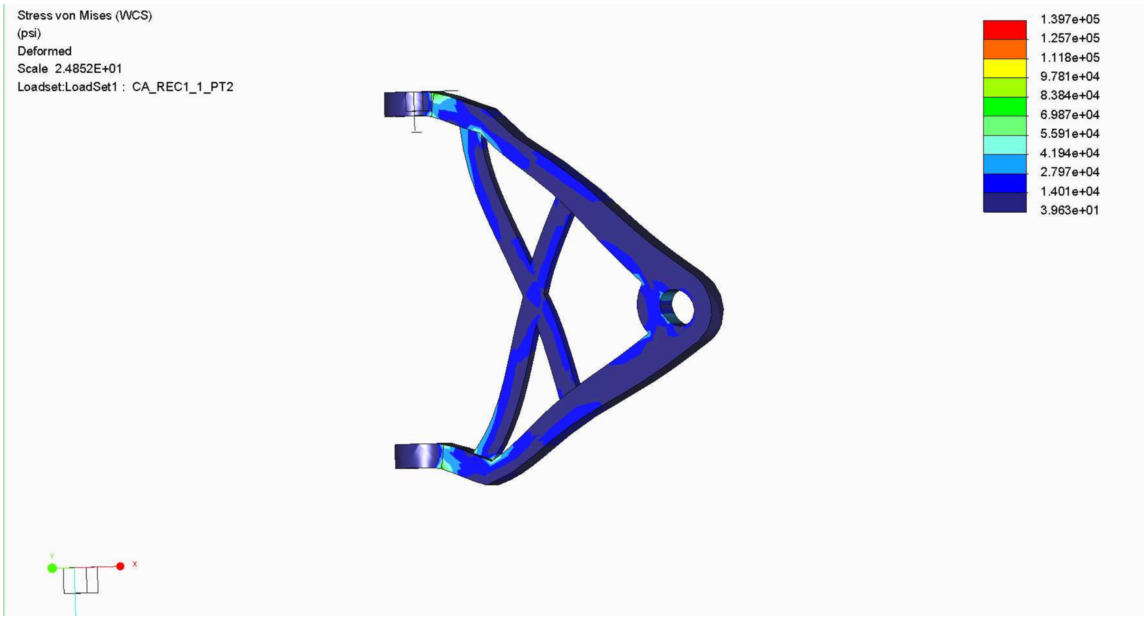

Figure 35 - 'X' Trajectory Rectangle I FEA Stress

The results of the stress analysis yielded a maximum von Mises stress of 1.397E5 psi. This is decreased from the same shape in the 'Z' trajectory, which produced a maximum von Mises stress of 1.786E5 psi. It is also less than the stresses of 1.773E5 psi and 1.784E5 psi which occurred in the unbraced steel and aluminum arms respectively. However as with the 'Z' trajectory there still exists a region with concentrated stress near the arms mounting locations.

4.2.1.2 Strains

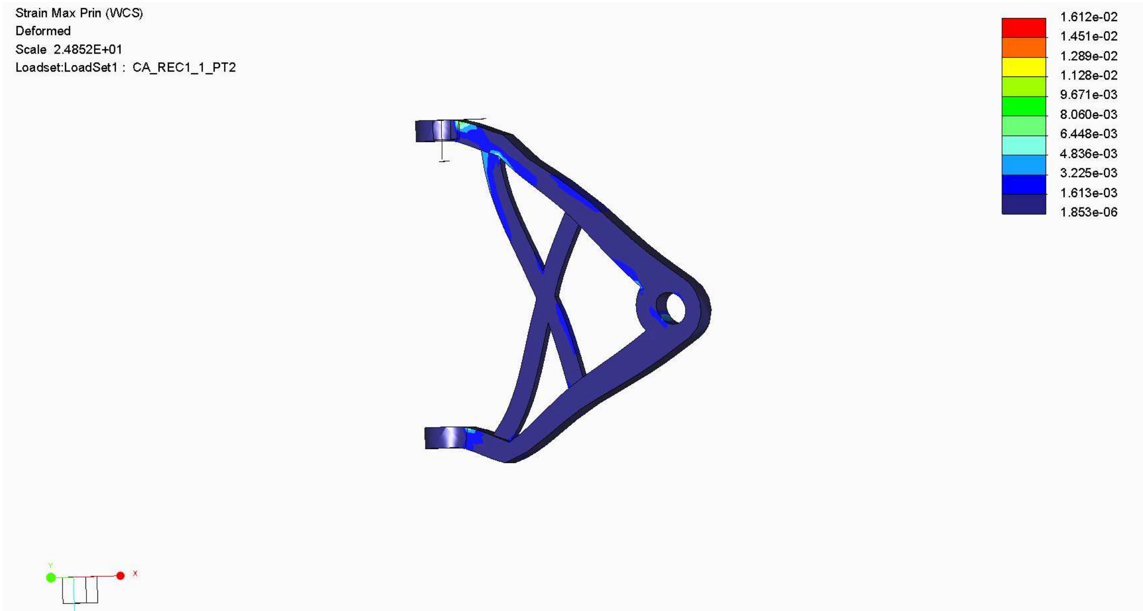

Figure 36 - 'X' Trajectory Rectangle I FEA Strain

As was done in the previous stage the stress analysis was then preceded by a FEA of the maximum principal strain. The strain analysis showed similar results to those of the stress analysis. The strain at the mounting locations was decreased when compared to the results of rectangle I in the first stage of this study. The strain was also decreased when compared to the unbraced aluminum arm, although, it managed to be increased from that of the unbraced steel arm. The FEA results showed that the bracing members became strained as well; these results can be observed in Figure 36. The outer members of the arms were relieved of some of the strains they had experienced before the addition of the cross bracing.

4.2.1.3 Deformations

Following the strain study, the displacement produced by this arm was also evaluated using the FEA capabilities of Pro-Engineer. The results of the displacement study can be observed in Figure 37. Under the 3500lb load, the rectangle I arm produced a maximum displacement of 0.0253 in. That is a decrease in deflection when compared to unbraced aluminum arm. These results are also close to the maximum displacement observed in the FEA study of the unbraced steel arm, which produced a displacement of 0.0214 in. The results are favorable in showing that an aluminum control arm utilizing this type of bracing can resist deflections nearly as well as steel control arm.

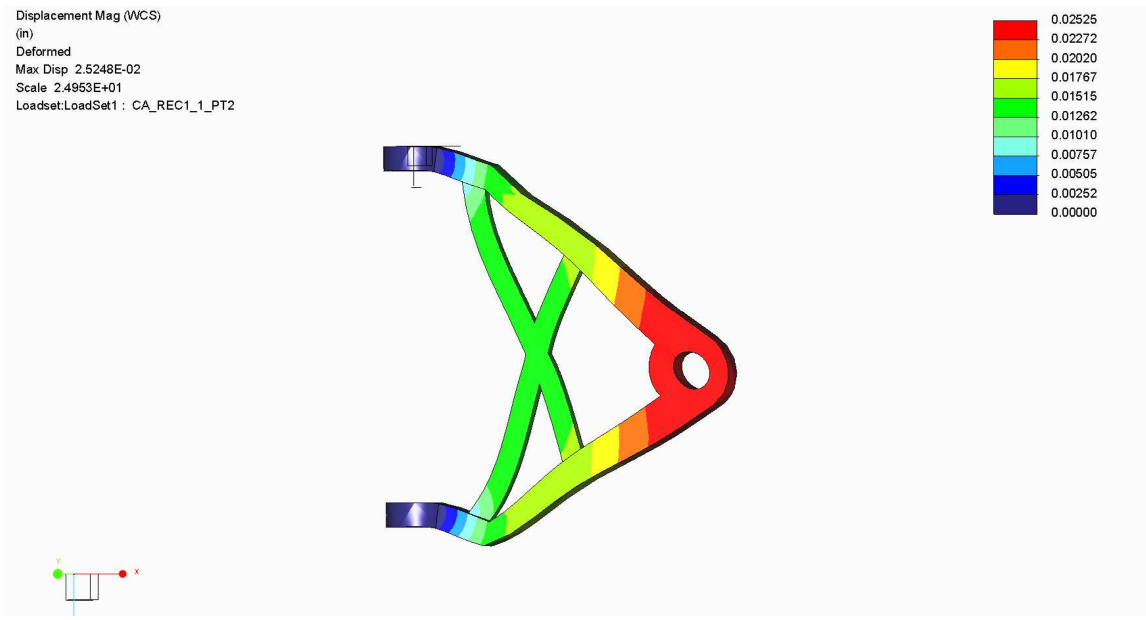

Figure 37 - 'X' Trajectory Rectangle I FEA Displacement

The maximum deflection that occurred was only slightly larger than that produced by the unbraced steel arm. This is despite the further reduction in displacement when compared to the unbraced aluminum arm and most of those studied in stage I. In addition to the FEA studies, the rectangle I arm, was also manufactured and tested experimentally. The arm was tested following the same procedure outlined in the previous experimental tests. As was observed in the previous studies, the maximum deflection when subjected to a 3500 lbs. load did not agree with the FEA study. This is again believed to be for the same reasons as were mentioned before. The FEA study showed a maximum deflection of approximately 0.0253 in while the experimental results showed to produce deflections in the range of 0.08 in. The graphed results from the experimental test can be viewed in Figure 38. The difference in these results is similar to the differences noticed in the results of the previous arms.

The rectangle I arm managed to produce a relatively smooth load vs. deflection curve. The curve shows that the arm failed quite suddenly as was seen with most of the previously studied arms. The peak load with which the rectangle I arm was able to with stand shows to be approximately 6400 lbs. This peak load is approximately 2000 lbs more than the same shape following the 'Z' trajectory. That is a 44% increase in maximum load with which the arm can with stand. This peak load is significantly greater than that of any previously studied arms. This particular arm was tested using two identical samples to ensure the results were repeatable. The two specimens produced identical curves confirming that the data was repeatable for multiple samples.

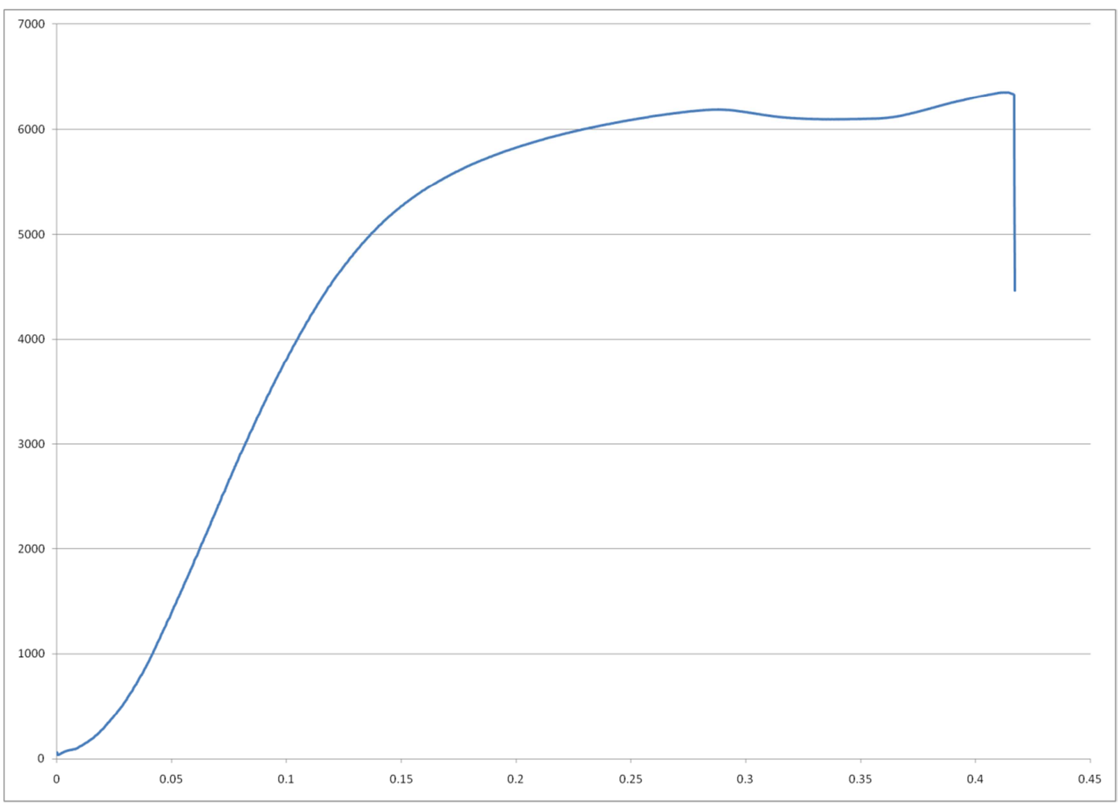

Figure 38 - 'X' Trajectory Rectangle I Load vs. Deflection Graph

4.2.2 Webbed Arm – Square Cross Section

The square cross section used to follow the new ‘X’ trajectory was identical to the square cross section used in stage I. The shape utilized the same dimensions and cross sectional area used before.

4.2.2.1 Stresses

To continue evaluating the effectiveness of bracing members following an 'X' trajectory the square shape was used. The first step in evaluating the square shape following the 'X' trajectory was to perform an FEA study. The study was performed in the same manner as was used in the previous shapes and arms of stage I. Figure 39 shows the results obtained in the stress analysis of the square shaped bracing members. The results show that the maximum von Mises stress that occurred was decreased from both that of the unbraced arm and the same shape in the 'Z' trajectory. It can also be seen that now both of the center members of the cross bracing are experiencing stress. Similarly, to the previous square shape and 'Z' trajectory the bracing members are redistributing the applied load. However, in the 'X' configuration the bracing members appear to be evenly taking on portions of the stress that once occurred in the arms outer elements. These results are comparable to those seen in the previous study of rectangle I following the shape 'X' shaped trajectory.

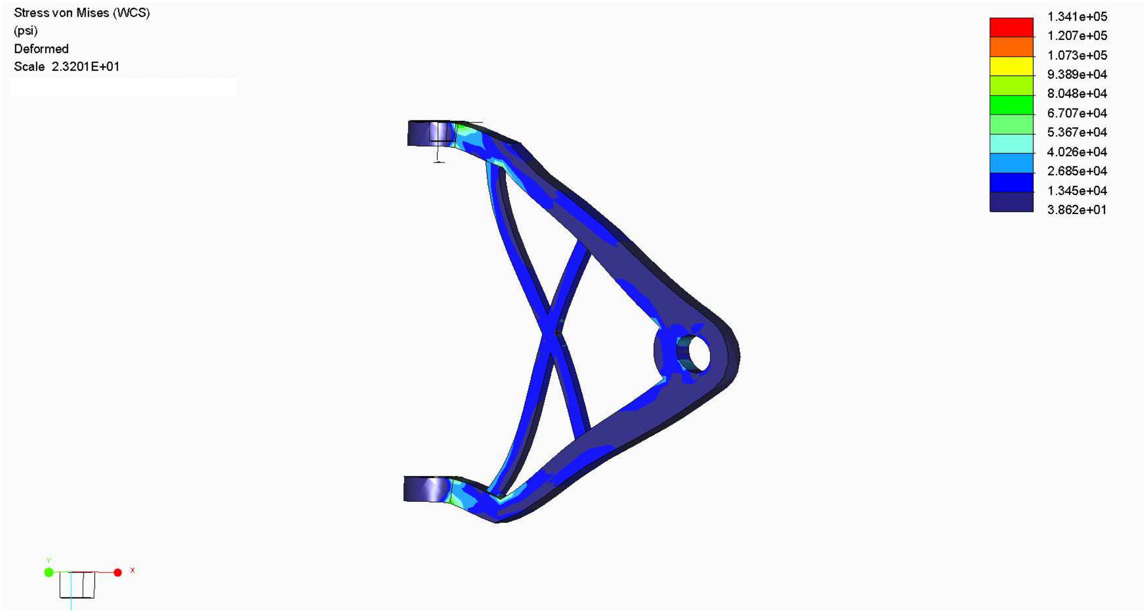

Figure 39 - 'X' Trajectory Square FEA Stress

4.2.2.2 Strains

As done in the previous studies the stress analysis was then preceded by a FEA of the maximum principal strain. The strain analysis showed similar results to those of the stress analysis. The strain at the mounting locations was decreased when compared to the results of the square shape in the first stage of this study. The strain was also decreased when compared to the unbraced aluminum arm, although, it managed to be increased from that of the unbraced steel arm. The FEA results showed that the bracing members became strained as well; these results can be observed in Figure 40. The outer members of the arms were relieved of some of the strains they had experienced before the addition of the bracing members.

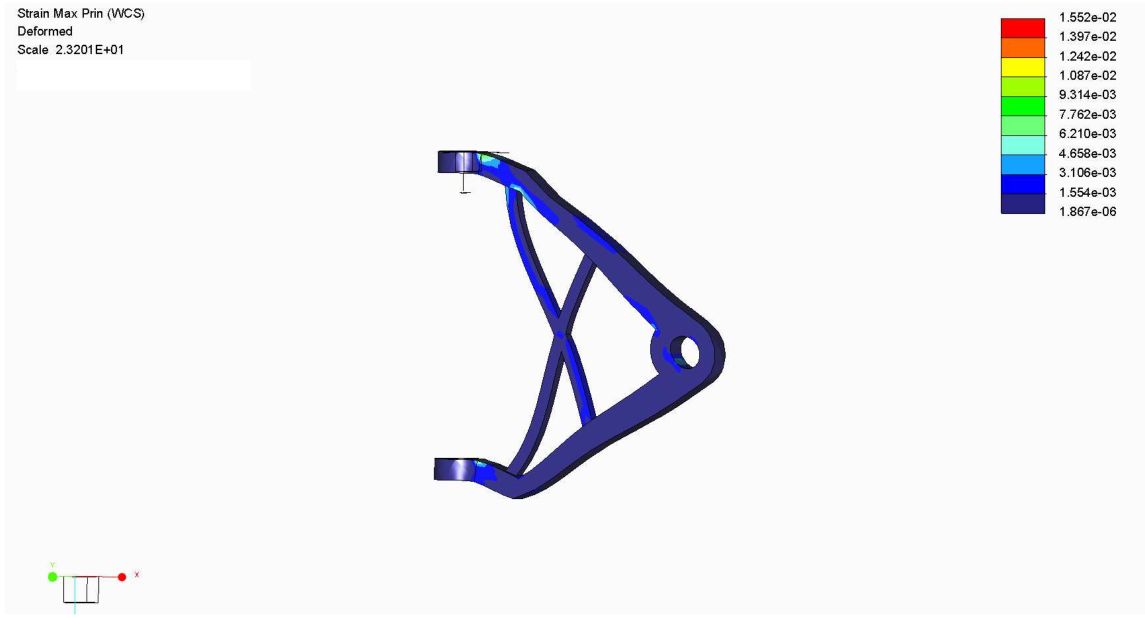

Figure 40 - 'X' Trajectory Square FEA Strain

4.2.2.3 Deformations

Following the strain study, the displacement produced by this arm was also evaluated using the FEA capabilities of Pro-Engineer. The results of the displacement study can be observed in Figure 41. Under the 3500 lb load, the square arm produced a maximum displacement of 0.0272 in. That is a decrease in deflection when compared to unbraced aluminum arm. These results are also close to the maximum displacement observed in the FEA study of the unbraced steel arm, which produced a displacement of 0.0214 in. The results are favorable in showing that an aluminum control arm utilizing this type of bracing can resist deflections nearly as well as steel control arm.

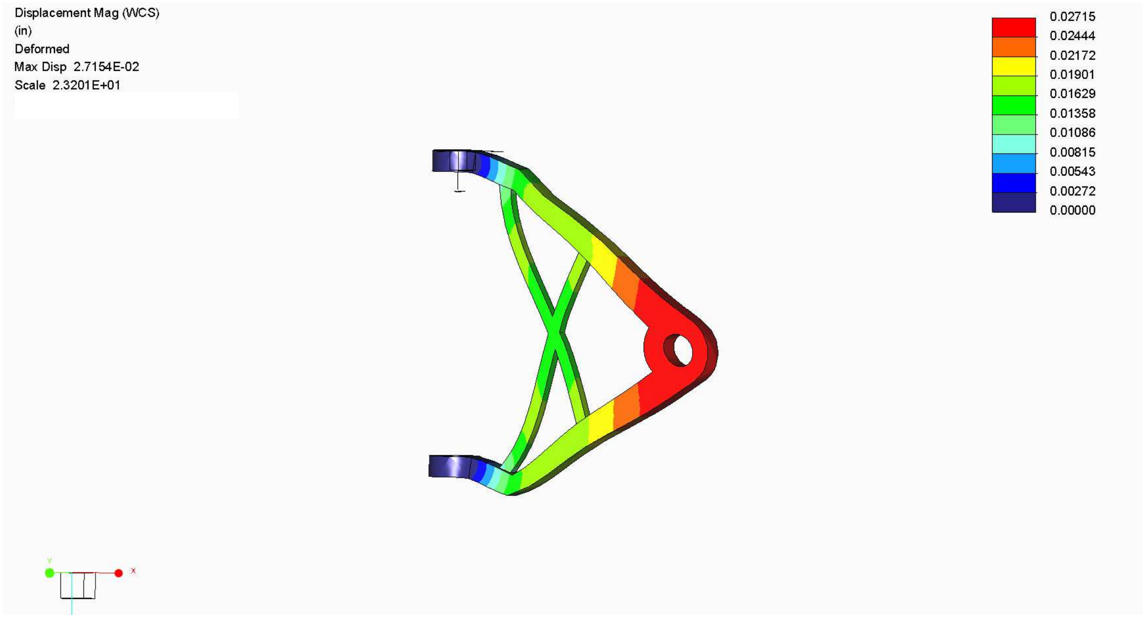

Figure 41 - 'X' Trajectory Square FEA Displacement

4.2.3 Webbed Arm - Rectangle II Cross Section

The rectangle II cross section used to follow the new ‘X’ trajectory was identical to the rectangular cross section used in stage I. The shape utilized the same dimensions and cross sectional area used before.

4.2.3.1 Stresses

To continue evaluating the effectiveness of bracing members following an 'X' trajectory the rectangle II shape was used. The first step in evaluating the rectangle II shape following the 'X' trajectory was to perform an FEA study. The study was performed in the same manner as was used in the previous shapes and arms of stage I. Figure 42 shows the results obtained in the stress analysis of the rectangle II shaped bracing members. The results show that the maximum von Mises stress that occurred was decreased from both that of the unbraced arm and the same shape in the 'Z' trajectory. These results are similar and in agreement with the previous shape following the 'X' trajectory. It can also be seen that now both of the center members of the cross bracing are experiencing stress. Similarly, to the previous rectangle II shape and 'Z' trajectory the bracing members are redistributing the applied load. However, in the 'X' configuration the bracing members appear to be evenly taking on portions of the stress that once occurred in the arms outer elements. These results are comparable to those seen in the previous studies following the 'X' shaped trajectory.

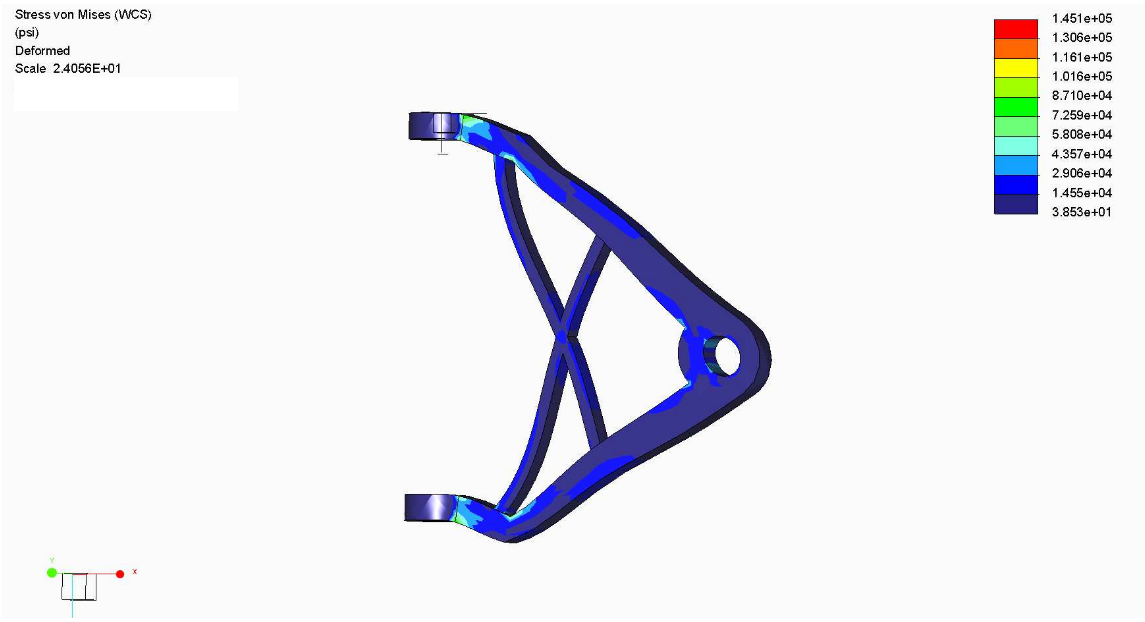

Figure 42 - 'X' Trajectory Rectangle II FEA Stress

4.2.3.2 Strains

As done in the previous studies the stress analysis was then preceded by a FEA of the maximum principal strain. The strain analysis showed similar results to those of the stress analysis. The strain at the mounting locations was decreased when compared to the results of the rectangle II shape in the first stage of this study. The strain was also decreased when compared to the unbraced aluminum arm, although, it managed to be increased from that of the unbraced steel arm. The FEA results showed that the bracing members became strained as well; these results can be observed in Figure 43. The outer members of the arms were relieved of some of the strains they had experienced before the addition of the bracing members.

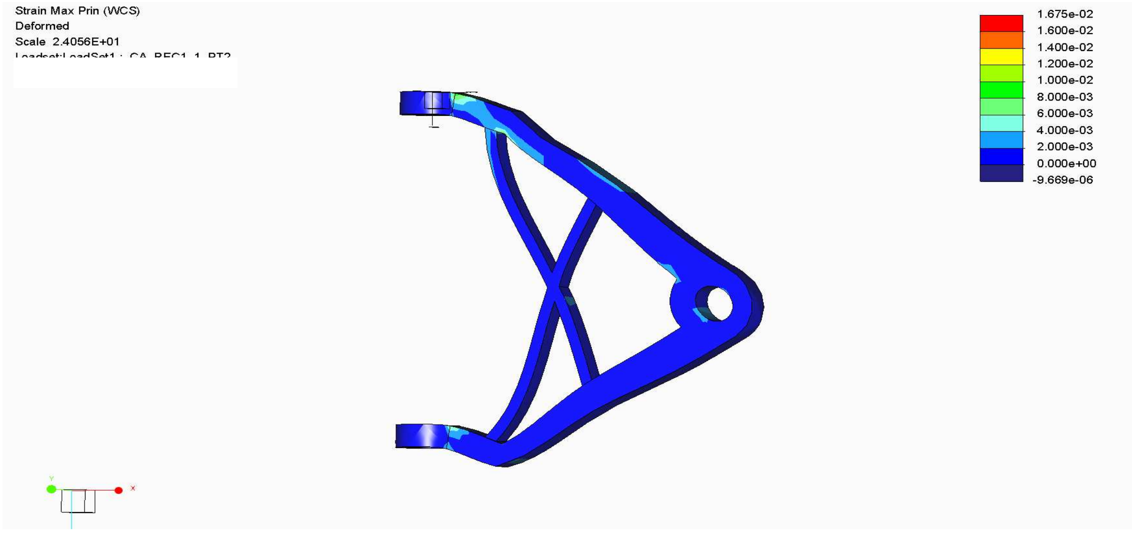

Figure 43 - 'X' Trajectory Rectangle II FEA Strain

4.2.3.3 Deformations

Following the strain study, the displacement produced by this arm was also evaluated using the FEA capabilities of Pro-Engineer. The results of the displacement study can be observed in Figure 44. Under the 3500lb load, the rectangle II arm produced a maximum displacement of 0.0262 in. That is a decrease in deflection when compared to unbraced aluminum arm. These results are also close to the maximum displacement observed in the FEA study of the unbraced steel arm, which produced a displacement of 0.0214 in. The results are favorable in showing that an aluminum control arm utilizing this type of bracing can resist deflections nearly as well as steel control arm.

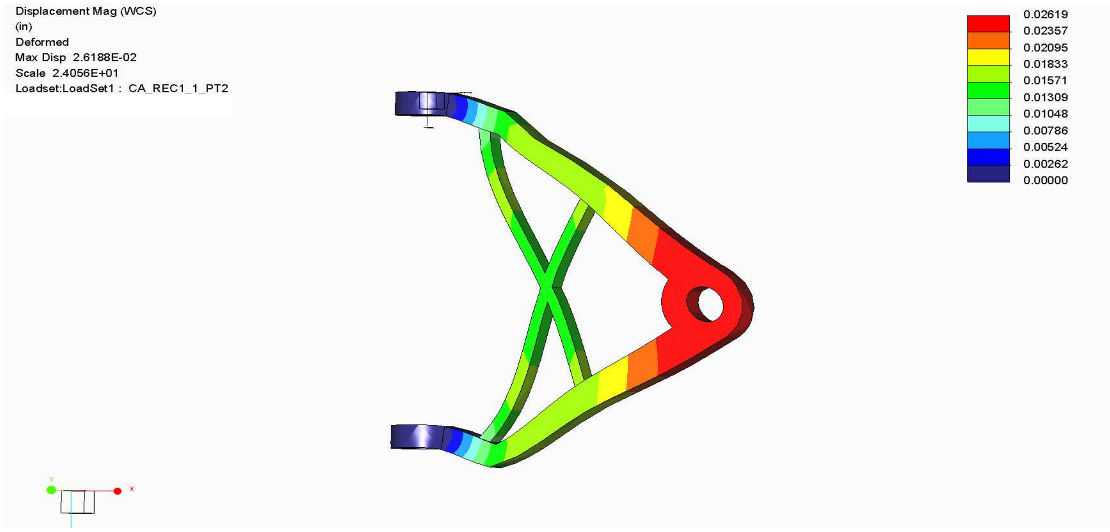

Figure 44 - 'X' Trajectory Rectangle II FEA Displacement

4.2.4 Other Web Cross Sectional Shapes

To maintain consistency, the additional shapes from stage I that were only studied using the FEA will also be studied in stage II. These shapes will serve for comparison with those from stage I. These shapes will be continued to be studied in the same manner, as were all of the previous arms. The cross sectional areas of the bracing member were also continued to be help constant.

4.2.4.1 Triangular Cross Sectional Web

The Triangular cross section used to follow the new ‘X’ trajectory was identical to the triangular cross section used in stage I. The shape utilized the same dimensions and cross sectional area used before.

4.2.4.1.1 Stresses

To continue evaluating the effectiveness of bracing members following an 'X' trajectory the triangle shape was used. The first step in evaluating the triangle shape following the 'X' trajectory was to perform an FEA study. The study was performed in the same manner as was used in the previous shapes and arms of stage I. Figure 45 shows the results obtained in the stress analysis of the triangle shaped bracing members. The results show that the maximum von Mises stress that occurred was decreased from both that of the unbraced arm and the same shape in the 'Z' trajectory. This result is similar and in agreement with the previous shapes following the 'X' trajectory. It can also be seen that now both of the center members of the cross bracing are experiencing stress. Similarly, to the previous triangle shape and 'Z' trajectory, the bracing members are redistributing the applied load. However, in the 'X' configuration the bracing members appear to be evenly taking on portions of the stress that once occurred in the arms outer elements. These results are comparable to those seen in the previous studies following the 'X' shaped trajectory.

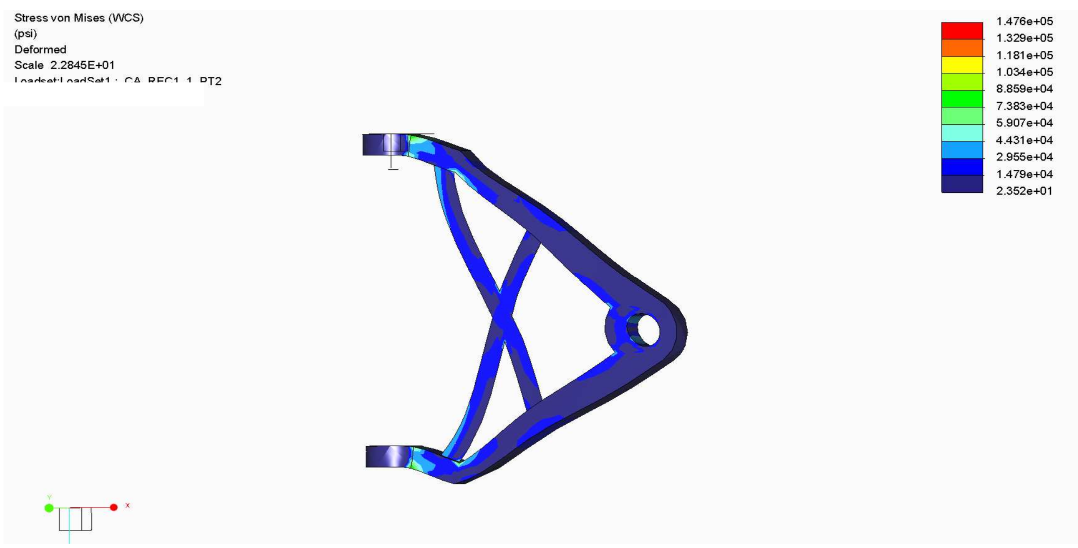

Figure 45 - 'X' Trajectory Triangle FEA Stress

4.2.4.1.2 Strains

As done in the previous studies the stress analysis was then preceded by a FEA of the maximum principal strain. The strain analysis showed similar results to those of the stress analysis. The strain at the mounting locations was decreased when compared to the results of the triangle shape in the first stage of this study. The strain was also decreased when compared to the unbraced aluminum arm, although, it managed to be increased from that of the unbraced steel arm. The FEA results showed that the bracing members became strained as well; these results can be observed in Figure 46.

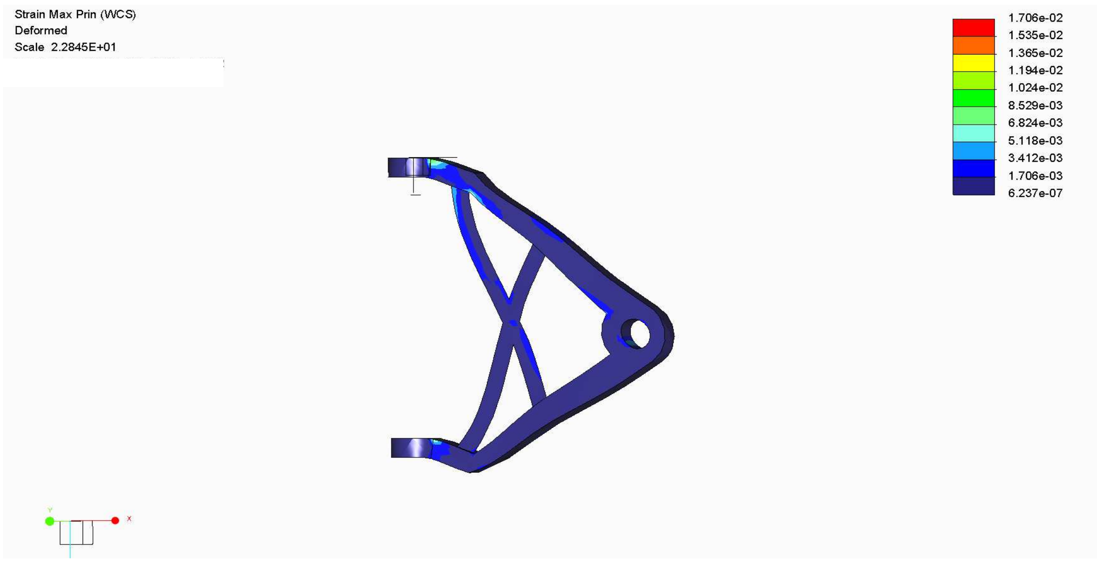

Figure 46 - 'X' Trajectory Triangle FEA Strain

4.2.4.1.3 Deformations

Following the strain study, the displacement produced by this arm was also evaluated using the FEA capabilities of Pro-Engineer. The results of the displacement study can be observed in Figure 47. Under the 3500lb load, the triangular arm produced a maximum displacement of 0.0276 in. That is a decrease in deflection when compared to unbraced aluminum arm. These results are also close to the maximum displacement observed in the FEA study of the unbraced steel arm, which produced a displacement of 0.0214 in. The results are favorable in showing that an aluminum control arm utilizing this type of bracing can resist deflections nearly as well as a steel control arm.

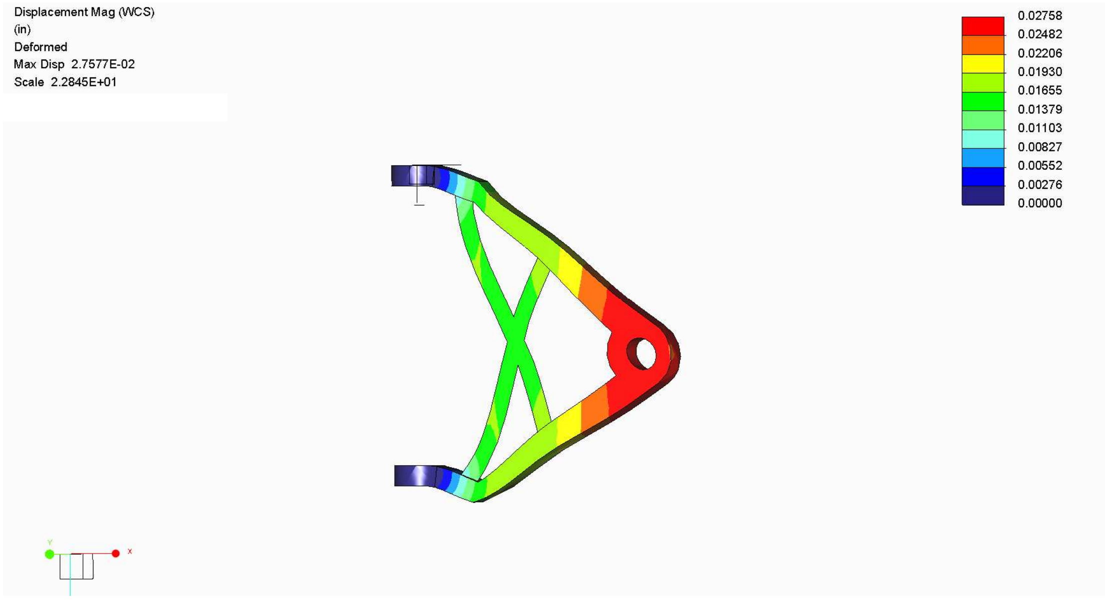

Figure 47 - 'X' Trajectory Triangle FEA Displacement

4.2.4.2 Circular Cross Sectional Web

The circular cross section used to follow the new ‘X’ trajectory was identical to the circular cross section used in stage I. The shape utilized the same dimensions and cross sectional area used before.

4.2.4.2.1 Stresses

To continue evaluating the effectiveness of bracing members following an 'X' trajectory the circular shape was used. The first step in evaluating the circular shape following the 'X' trajectory was to perform an FEA study. The study was performed in the same manner as was used in the previous shapes and arms of stage I. Figure 48 shows the results obtained in the stress analysis of the circular shaped bracing members. The results show that the maximum von Mises stress that occurred was decreased from both that of the unbraced arm and the same shape in the 'Z' trajectory. This result is similar and in agreement with the previous shapes following the 'X' trajectory. It can also be seen that now both of the center members of the bracing are experiencing stress. Similarly, to the previous circular shape and 'Z' trajectory, the bracing members are redistributing the applied load. However, in the 'X' configuration the bracing members appear to be evenly taking on portions of the stress that once occurred in the arms outer elements. These results are comparable to those seen in the previous studies following the 'X' shaped trajectory.

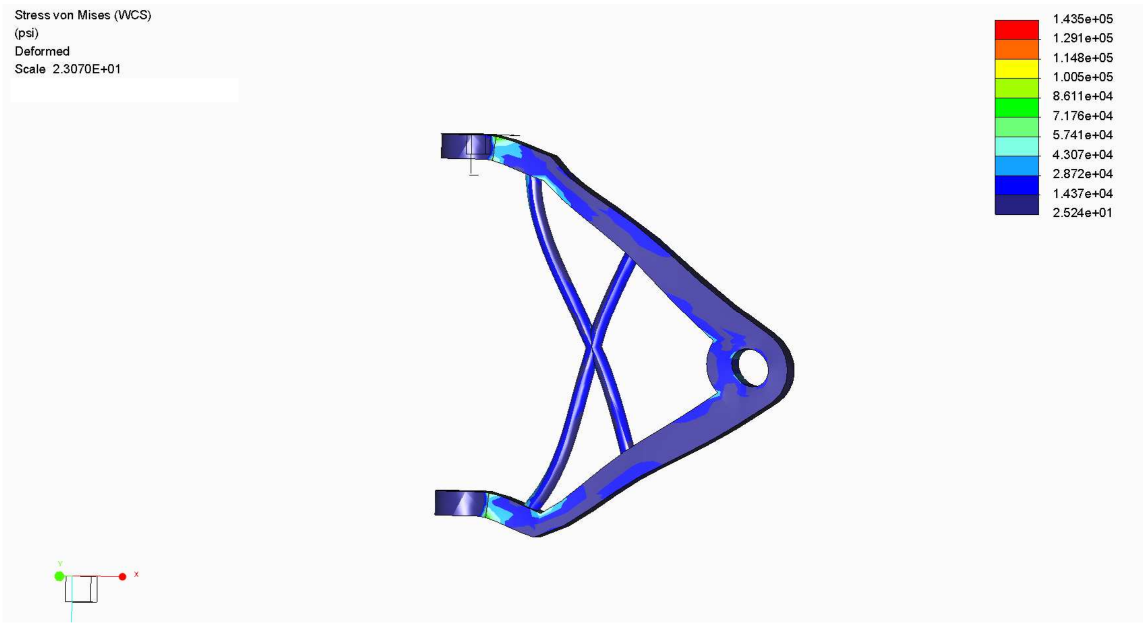

Figure 48 - 'X' Trajectory Circle FEA Stress

4.2.4.2.2 Strains

As done in the previous studies the stress analysis was then preceded by a FEA of the maximum principal strain. The strain analysis showed similar results to those of the stress analysis. The strain at the mounting locations was decreased when compared to the results of the circular shape in the first stage of this study. The strain was also decreased when compared to the unbraced aluminum arm, although, it managed to be increased from that of the unbraced steel arm. The FEA results showed that the bracing members became strained as well; these results can be observed in Figure 49.

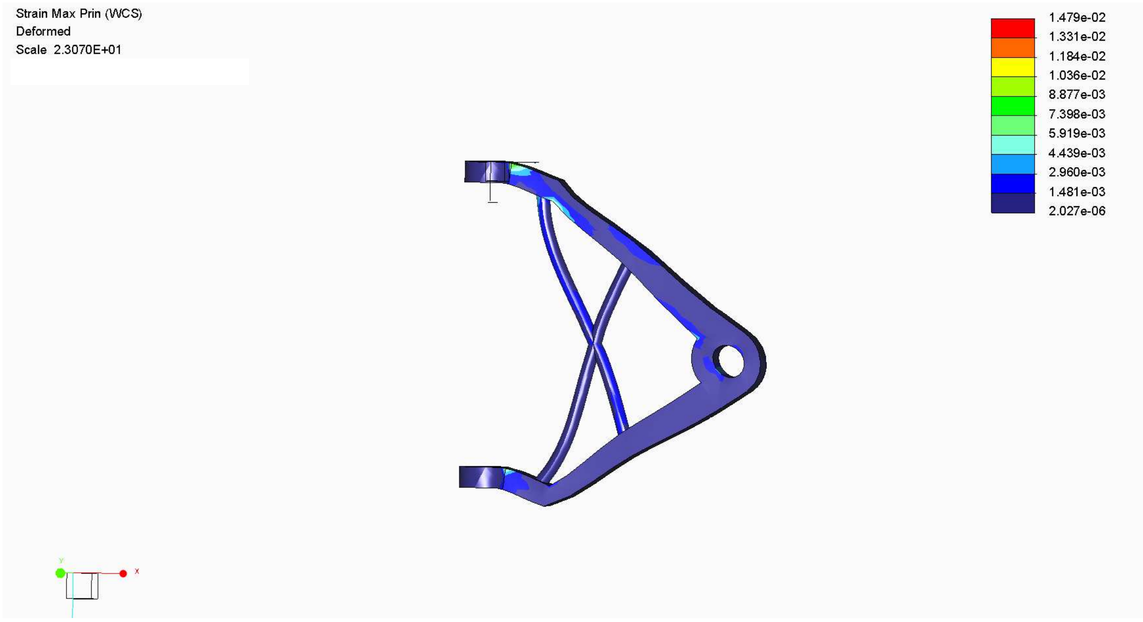

Figure 49 - 'X' Trajectory Circle FEA Strain

4.2.4.2.3 Deformations

Following the strain study, the displacement produced by this arm was also evaluated using the FEA capabilities of Pro-Engineer. The results of the displacement study can be observed in Figure 50. Under the 3500lb load, the circular arm produced a maximum displacement of 0.0273 in. That is a decrease in deflection when compared to unbraced aluminum arm. These results are also close to the maximum displacement observed in the FEA study of the unbraced steel arm, which produced a displacement of 0.0214 in. The results are favorable in showing that an aluminum control arm utilizing this type of bracing can resist deflections nearly as well as a steel control arm.

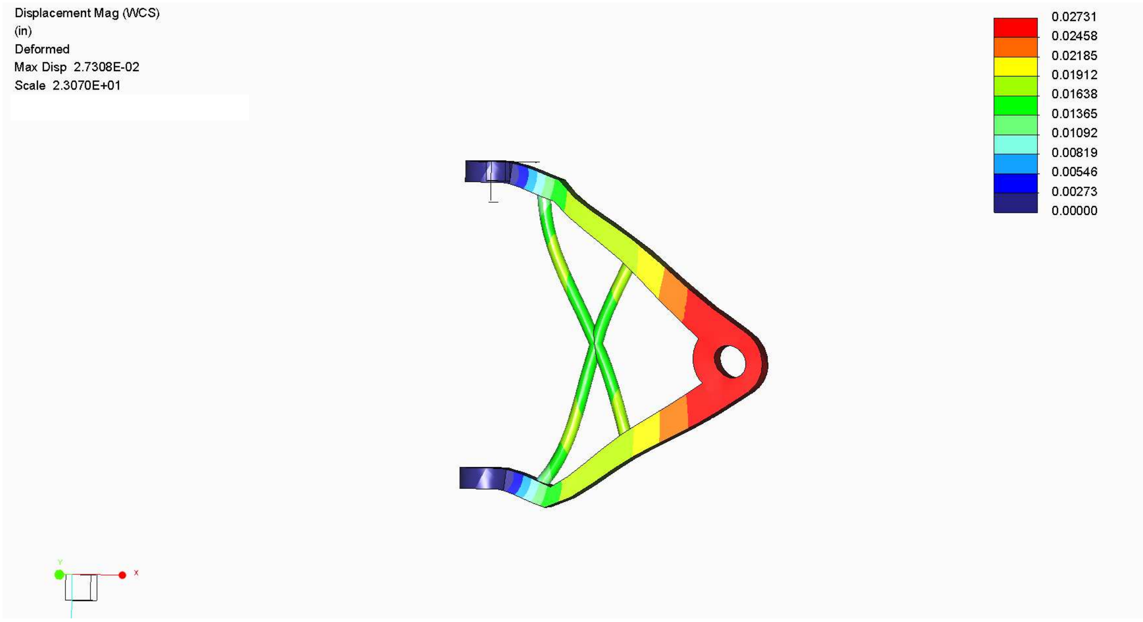

Figure 50 - 'X' Trajectory Circle FEA Displacement

Chapter 5: Conclusions

The results from of both phases of this study are summarized. The results from both the FEA's and the physical experiments are compared in order to draw conclusions about the effects the bracing has on deflections of control arms. The data displayed in Table 1 shows the maximum deflections occurring in each of the control arms used in this study. As mentioned, the arms utilizing the 'X' shaped trajectory deflected less than those which used the 'Z' shaped trajectory. The 'X' shaped arms that were experimentally tested also withstood higher load for the same deformation.

	Maximum Experimental Displacement at (in):				Maximum FEA Displacement at (in):		
Control Arm	**3000 Lbf**	**3500 Lbf**	**4000 Lbf**	**4500 Lbf**		**3500 Lbf**	
Original Unbraced Arm (1020)	N/A	N/A	N/A	N/A		0.0214	
Original Unbraced Arm (6061)	0.1118	0.1395	0.2072	0.4844		0.062	
Stage I, 'Z' Trajectory							
Rectangle I	0.0776	0.0919	0.1223	0.4698		0.0365	
Rectangle II (1)	0.1245	0.1418	0.1659	0.2221		0.0392	
Rectangle II (2)	0.1082	0.1236	0.1422	0.1698		0.0392	
Square	0.0709	0.0863	0.1192	.2120*		0.038	
Stage II, 'X' Trajectory							
Rectangle I (1)	0.082	0.0928	0.1047	0.1185		0.0253	
Rectangle I (2)	0.0735	0.0846	0.096	0.1091		0.0253	
Rectangle II	N/A	N/A	N/A	N/A		0.0262	
Square	N/A	N/A	N/A	N/A		0.0272	
Circle	N/A	N/A	N/A	N/A		0.0273	
Triangle	N/A	N/A	N/A	N/A		0.0276	

Table 1 – Maximum Deflections

Additional data for the arms which were tested physically can be found in Table 2. This data includes the maximum deflections and loads at which each arm failed. The respective weights of each arm are listed as well to create a comparison. It can be observed from the data in Table 2 that the 'X' shaped arms fell within the same weight range as the other braced arms, while also providing a significant increase in strength.

Control Arm	Weight (g):	Weight (Lbs):	Load at Failure (Lbf):	Displacement at Failure (in):
Original Unbraced Arm	130	0.2866	4155	1.0034
Stage I, 'Z' Trajectory				
Rectangle I	148	0.3263	4320	0.5438
Rectangle II (1)	165	0.3638	4430	0.2529
Rectangle II (2)	166	0.3660	4438	0.2773
Square	150	0.3307	4352	0.2121
Stage II, 'X' Trajectory				
Rectangle I (1)	156	0.3439	6331	0.4168
Rectangle I (2)	156	0.3439	6336	0.4014

Table 2 - Weight and Peak Load Data

The data shown in Table 3 displays the strength to weight ratios of all the arms that were manufactured and tested experimentally. The percentage weight increase from the unbraced aluminum control arm is also listed for comparative purposes. It can be seen from the data that the arms designed with the 'X' trajectory bracing yielded the highest strength to weight ratios. When compared to all of the other experimentally tested arms, the arms from stage II produced a significantly higher strength to weight ratio. This is achieved by a 20% increase in weight which was produced by the addition of the bracing members. Of all the arms tested, the arm with the second highest strength to weight ratio was surprisingly the unbraced arm.

Control Arm	Strenghth/Weight Ratio	Percentage weight increase:
Original Unbraced Arm	14497.53	0.00
Stage I, 'Z' Trajectory		
Rectangle I	13240.01	13.85
Rectangle II (1)	12178.28	26.92
Rectangle II (2)	12126.78	27.69
Square	13160.24	15.38
Stage II, 'X' Trajectory		
Rectangle I (1)	18408.31	20.00
Rectangle I (2)	18422.85	20.00

Table 3 – Strength to Weight Ratios and Percent Weight Increase

The data displayed in Table 4 shows the experimentally measured maximum principal strains compared to the FEA maximum principal strain. The data shown is not entirely in agreement; this is because of limitations in where the strains were monitored on the samples. The maximum principal strains as mentioned previously, occurs at the location of the mounting holes on the samples. Monitoring the strains at these points was not possible while conducting this study. The strain gauges were mounted as close to that location as possible; however, there still existed a large enough difference to create discrepancies in the data.

Control Arm	Maximum Principle Strain Experimental (ε)	Maximum Principle Strain FEA (ε)
Original Unbraced Arm (1020)	N/A	0.00660
Original Unbraced Arm (6061)	0.00931	0.01924
Stage I, 'Z' Trajectory		
Rectangle I	0.01606	0.02037
Rectangle II (1)	0.00375	0.02231
Square	0.002693	0.02067
Circle	N/A	0.04202
Triangle	N/A	0.00410
Stage II, 'X' Trajectory		
Rectangle I (1)	N/A	0.01612
Rectangle II	N/A	0.01675
Square	N/A	0.01552
Circle	N/A	0.01479
Triangle	N/A	0.01706

Table 4 - Maximum Principal Strains

It can be concluded that the addition of bracing members to control arms does reduce the deflections that occur. The deflections were decreased in most cases regardless of the cross section used in the bracing members. It is clear from the data that certain shapes will reduce deflections by a greater amount than others. Some particular shapes produced better results depending on what trajectory was used. Most importantly it can be concluded from this study that the trajectory chosen for the bracing members has a greater effect than the particular cross sectional shape used. Being that there is essentially an infinite number of possible configurations for bracing members the configurations discussed in this study were selected to provide proof of concept. When adding bracing members to a control arm structure, focus should be placed on the path for the bracing.

Difficulties associated in the manufacturing process should be considered when attempting to use or produce control arms with bracing members. These control arms should prove to be most applicable to lightweight hybrid vehicles. Design engineers working to produce lighter and stronger suspension components for hybrid or compact fuel efficient vehicles should consider the use of these arms. With additional studies and optimal design may be able to be selected. These arms are believed to also be applicable to competition automotive sport such as racing specifically open wheeled cars utilizing push rod suspension systems.

Lastly it needs to be stated that there are limitations to the results obtained in this study. It is clear that there were significant differences between the FEA and experimental results. The general trends recognized between the two were in agreement; however, the specific numerical values were not. The arms which deflected the most in the FEA did so in the experiment as well. The main source of the differences between these two results is due to the way in which Pro-Mechanica constrains the surface of the parts in the FEA.

Future studies should specifically investigate the trajectory of the bracing members and how they affect deflections. Those studies should expect limited convergence of the results if studied by both FEA and experimentally. The FEA results will produce a general trend that can be observed in the experimental results. The numerical values of the results will differ significantly. If this study was to be performed using larger scale parts it is expected that the results will be in a closer agreement.

References

[1] Bash A.M., 2011 “Design lower arm using optimum approach,” Modern Applied Science, **5**(1), pp. 56-67.

[2] Zhao T. and Jiang Y., 2008 “Fatigue of 7075-T651 aluminum alloy,” International Journal of Fatigue, **30**(5), pp. 834-849.

[3] Hu Q., McColl I.R., Harris S.J., and Waterhouse R.B., 2000 “The role of debris in the fretting wear of a SiC reinforced aluminum alloy matrix composite,” Wear, **245**(1), pp. 10-21.

[4] McColl I.R., Harris S.J., Hu Q., Spurr G.J., and Wood P.A., 1997 “Influence of surface and heat treatment on the fretting wear of an aluminum alloy reinforced with SiC particles,” Wear, **203-204**, pp. 507-515.

[5] Song B.C., 2009 "Structural optimization of an upper control arm, considering the strength, Proceedings of the Institution of Mechanical Engineers,” Journal of automobile engineering, **223**(6), pp.727-735.

[6] Kang W.J., Kim A.K., and Kim G.H., 2007 “Fatigue failure prediction of press fitted parts subjected to a cyclic loading condition by finite element methods,” Fatigue & Fracture of Engineering Materials & Structures, **30**(12), pp. 1194-1202.

[7] Kim Y., Yang S., Sohn H., Park J., and Choi S., 2006 “Finite element analysis to optimize forming conditions for lower control arm,” Metallurgical and Materials Transactions A., **37**(8), pp. 2539-2547.

[8] Taylor D.E. and Waterhouse R.B., 1971 “The effect of heat treatment on the fretting corrosion of a carbon steel,” Corrosion Science, **11**(11), pp. 833-842.

[9] Aldham D., Warburton J., and Pendlebury R.E., 1985 “The unlubricated fretting wear of mild steel in air,” Wear, **106**(1), pp. 177-201.

[10] Hanssen E., Vogt M., and Dilger K., 2012 “Fatigue assessment of arc welded automotive components using local stress approaches: Application to a track control arm, ”International Journal of Fatigue, **34**(1), pp. 57-64.

[11] Hyun C. and Kim H., 2010 “Fatigue properties of a modified 7075 aluminum alloy containing scandium,” Journal of Materials Science, **45**(11), pp. 3067-3072.

[12] Mirza N., Hussain K., Day A.J., and Klaps J., 2009 “Effect of component stiffness and deformation on vehicle lateral drift during braking". *Proceedings of the Institution of Mechanical Engineers, Part K,” Journal of Multi-body Dynamics,***223**(1), pp. 9-22.

[13] Tang L., Shangguan W., and Dai L., 2012 "A calculation method of joint forces for a suspension considering nonlinear elasticity of bushings. Proceedings of the Institution of Mechanical Engineers, Part K," Journal of Multi-body Dynamics, **226**(4), pp. 281-297.

[14] Bonakdar A., Wang F., Williams J.J., and Chawla N., 2012 "Environmental effects on fatigue crack growth in 7075 aluminum alloy," Metallurgical and Materials Transactions A., **43**(8), pp. 2799-2809.

[15] Haiba M., Barton D.C., Brooks P.C., and Levesley M.C., 2003 "The development of an optimization algorithm based on fatigue life," International Journal of Fatigue, **25**(4) pp. 299-310.

[16] Haiba M., Barton D.C, Brooks P.C., and Levesley M.C., 2002 "Review of life assessment techniques applied to dynamically loaded automotive components," Computers and Structures, **80**(4), pp. 481-494.

[17] Harris S.J., Overs M.P., and Gould A.J., 1985 "The use of coatings to control fretting wear at ambient and elevated temperatures," Wear, **106**(1), pp. 35-52.

[18] Ossa E.A., Palacio C.C., and Paniagua M.A., 2011 "Failure analysis of a car suspension system ball joint," Engineering Failure Analysis, **18**(5), pp. 1388-1394.

[19] Rohatgi P.K., Alaraj S., Thakkar R.B., and Daoud A., 2007 "Variation in fatigue properties of cast A359-SiC composites under total strain controlled conditions: Effects of porosity and inclusions," Applied Science and Manufacturing, **38**(8), pp. 1829-1841.

[20] Klaps J., and Day A.J., 2005 "Steering drift and wheel movement during braking: static and dynamic measurements," Journal of Automobile Engineering, **219**(1), pp. 11-19.

Appendix

A1 - Stage I Discussion of Failure

During stage I, several different cross sectional shapes were evaluated for their effectiveness in reducing deflections occurring in a control arms. The shapes all followed an arbitrary ‘Z’ shaped trajectory in order to provide proof of concept. The arms able to be manufactured and tested physically with the available machining applications were constructed from 6061 aluminum alloy. These arms were inserted into the specially designed testing apparatus and a continually increasing load was applied to the arms until failure occurred. Each arm failed similarly but with its own unique characteristics.

A1.1- Original Unbraced Arm (6061)

The first of the arms to be tested was the original unbraced aluminum arm. This arm was tested in a manner that provided a representation of the FEA as well as a vehicles sub-frame. The original unbraced arm was tested until failure occurred, during the testing the strains, load and deflection were monitored continuously. The failed unbraced arm can be observed in Figure 51. It can be seen that this arm deformed significantly before failing.

Figure 51 - Original Arm Failure

The unbraced aluminum arm completely failed only after deflecting approximately one inch. This arm was interesting to study because it failed in manner that was not expected. The arm failed by beginning to tear and shear off near the location of where the load was applied. Failure in this manner was unexpected because that portion of the arm is where the most material existed. Before performing the experiment on the unbraced arm, it was expected to fail near the mounting location. The results of the failure from the experimental specimen can be observed in Figure 52. It can be seen that the arm began to fail up and to the left of the hole where the load was applied. The pin joint hole is representative of a ball joint mounting location in a vehicles suspension system. The testing of this arm was stopped at this point because the load decreased from the maximum by greater than 25%. As mentioned previously a reduction in loading of this magnitude was defined to be considered a failure.

Figure 52 - Original Arm Fracture

A1.2 - Square

The next of the arms to be tested was the square arm. This arm was tested in the same manner as the previous unbraced arm. The square arm was tested until failure occurred; similarly, the strain, load and deflection were monitored continuously. The failed square arm can be observed in Figure 53.

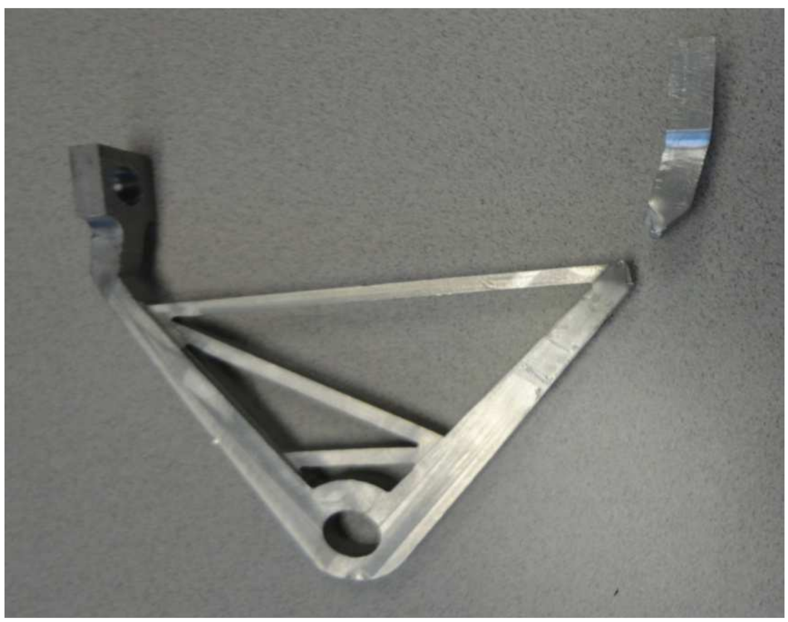

Figure 53 - Square Fracture (1)

The square arm failed by completely shearing off. The location of the failure is favorably close to the locations where the FEA showed to have increased strains and stress. It can also be observed that this arm did in fact deform; however, the level of deformation is significantly less than observed in the unbraced arm.

Figure 54 - Square Fracture (2)

The failure of the square arm can be observed in Figure 54. The figures show telltale signs of how the arm failed. It can be observed in this figure that the failure occurred at the base of a bracing member. It appears that the characteristics of the failed area, was influenced by the shape of the cross section used in the bracing members. There is a, roughly speaking, visible square shape within the cross section of the fractured area. It can also be observed from Figure 54 as if the failure propagated from around the edges of where the bracing elements connect with the outer portion of the arm.

A1.3 - Rectangle I

The next of the arm to be tested was the rectangular I arm. This arm was tested in the identical manner as the previous arms. The rectangle I arm was tested until failure occurred; similarly, the strain, load and deflection were monitored continuously. The failed rectangle I arm can be observed in Figure 55.

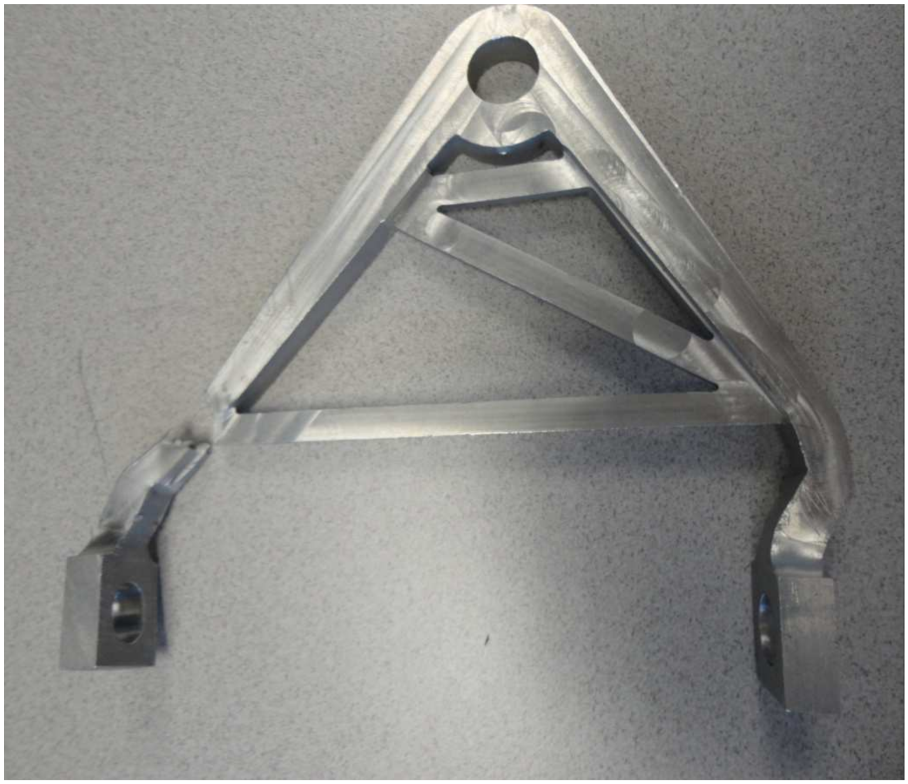

Figure 55 - Rectangle I Fracture (1)

Similar to square arm, the rectangle I arm failed by completely shearing off. The location of the failure is favorably close to the location where the FEA showed to have increased strains and stress. It is also observed that this arm that this arm did in fact deform; however, the level of deformation is again significantly less than was observed in the unbraced arm. As was noticed with the square arm, the fracture of this arm occurred at the same point where a bracing member connected to the main structure of the arm. The overall deformation of the rectangular I arm is comparable to that of the square arm. However, the fractured area of the rectangle I arm produced unique results. These results can be observed in Figure 56 and Figure 57.

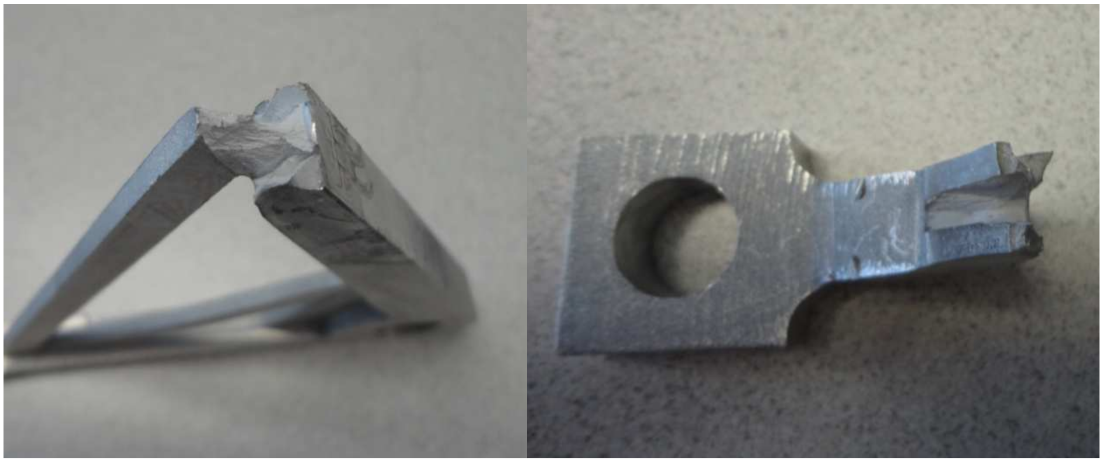

Figure 56 - Rectangle I Fracture (2)

The fractured area of the rectangle I arm shows different results than what were observed in the square arm. In Figure 46, it can be noticed that the fracture appears to have developed around the intersection of the bracing member sand the main structure of the control arm. As was noticed in the square arm the fractured area shows the influence of the bracing members by revealing a rectangular shape in fractured area. However, this fractured area is different from what was observed in the square arm. In this arm, it can be seen that a continuation of the rectangular bracing was torn out of the main structure.

Figure 57 - Rectangle I Fracture (3)

The failure of the rectangle I arm is also unique because it revealed that the arm was simultaneously failing at two points relatively close to one another. Figure 57 shows that the arm had begun failing at another location which is closer to the mounting holes; this was not observed in the square arm failure. Another unique characteristic of this arms failure can be seen in Figure 58. This figure shows that the center-bracing member actually buckled during the test and began deflecting outward. This result agrees with that of the FEA study performed previously. It shows that the center-member was under stress. It also shows that this member was aiding in the redistribution of the applied load to different portions of the control arms structure. It is also observed that the buckling occurred in the direction in which the shape has its least area moment of inertia.

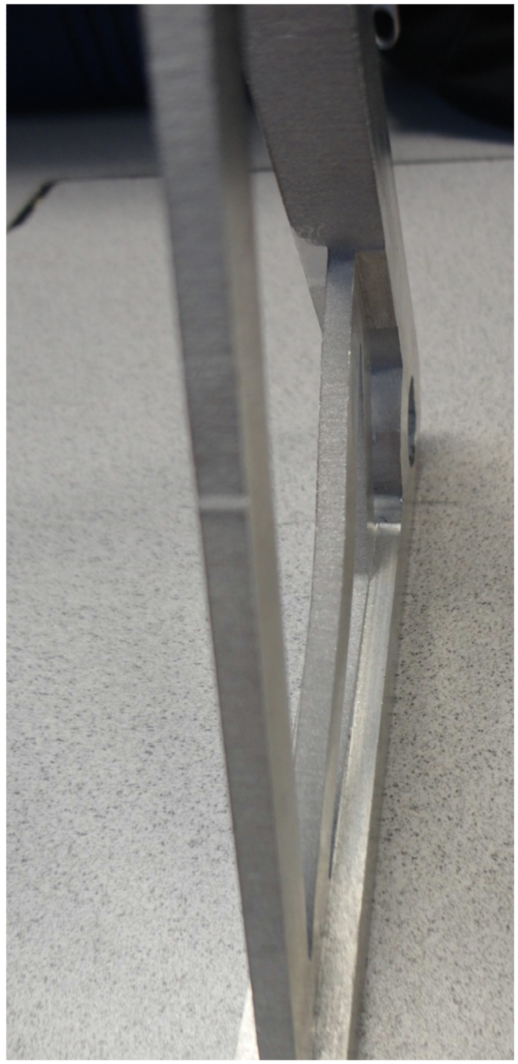

Figure 58 - Rectangle I Fracture (4)

A1.4 - Rectangle II

The next of the arm to be tested was the rectangular II arm. This arm was tested in the identical manner as the previous arms. The rectangle II arm was tested until failure occurred; similarly, the strain, load and deflection were monitored continuously. The failed rectangle II arm can be observed in Figure 59.

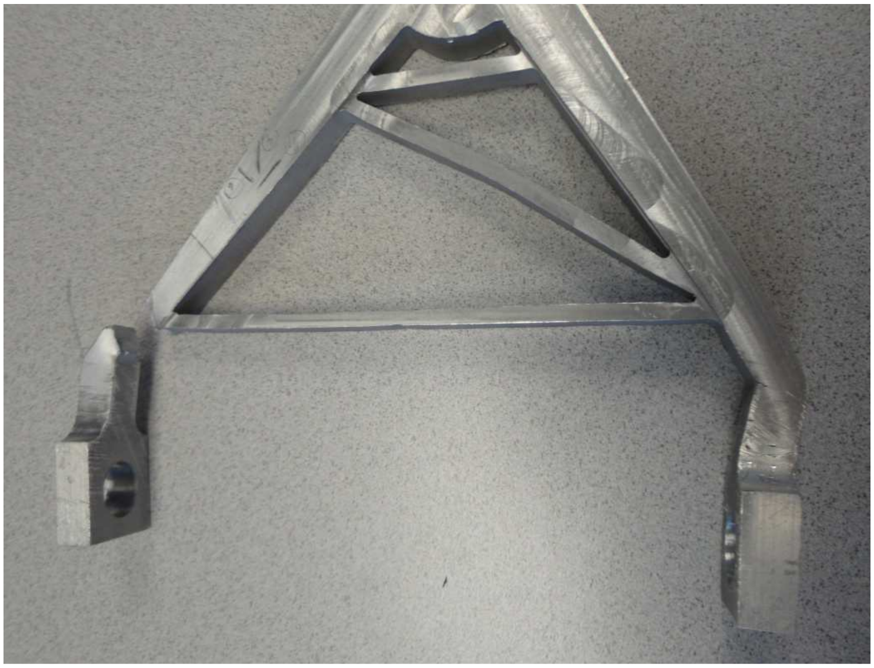

Figure 59 - Rectangle II Fracture (1)

Similar to the previous braced arms, the rectangle I arm failed by completely shearing off. The location of the failure is favorably close to the location where the FEA showed to have increased strains and stress. It is also observed that this arm did in fact deform; however, the level of deformation is again significantly less than was observed in the unbraced arm. As was noticed with the previous braced arms, the fracture of this arm occurred at the same point where a bracing member connected to the main structure of the arm. The overall deformation of the rectangular II arm is comparable to that of the other braced arms. However, the fractured area of the rectangle I arm produced unique results. These results can be observed in Figure 60 and Figure 61.

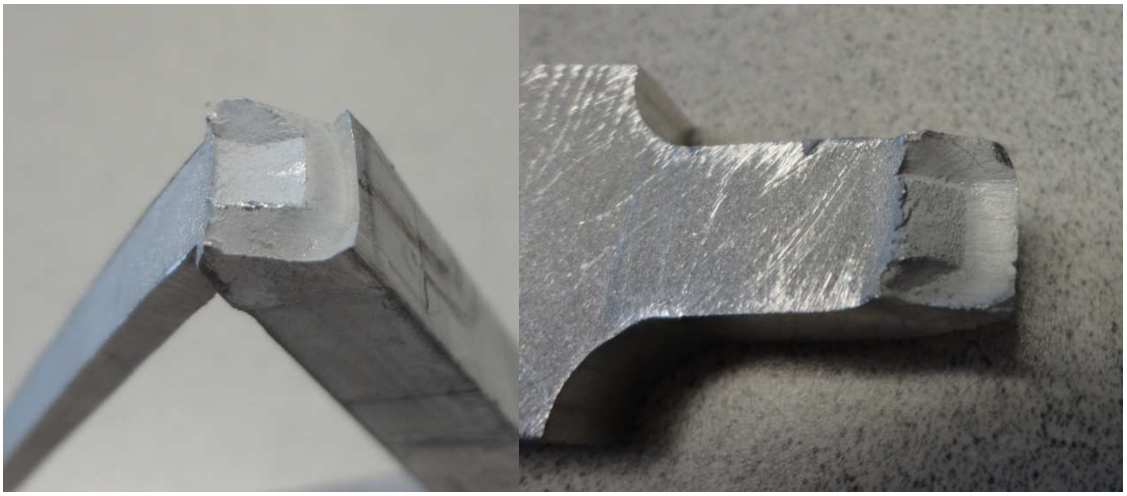

Figure 60 - Rectangle II Fracture (2)

The fractured area of the rectangle I arm shows different results than what were observed in the rectangle I arm. However, the results are comparable with those of the square arm. In Figure 60, it can be noticed that the fracture appears to have developed around the intersection of the bracing member and the main structure of the control arm. As was noticed in the square arm the fractured area reveals the influence of the bracing members by producing a rectangular shape in fractured area. This fractured area is comparable with what was observed in the square arm, although, it is significantly different than was observed in rectangle I.

The failure of the rectangle II arm is comparable to that of the rectangle I arm in that it shows the center-bracing member buckled during the test and began deflecting. This result agrees with that of the FEA study performed, it shows that the center-member was under stress. It also shows that this member was aiding in the redistribution of the applied load to different portions of the control arms structure. It is again observed that the buckling occurred in the direction in which the shape has its least area moment of inertia.

Figure 61 - Rectangle II Buckling (3)

A1.5 - Other Shapes

To conclude the discussion of failures observed in stage I it is essential to briefly mention the results of the sample test pieces. One of these test pieces includes what would have been an arm utilizing triangular shaped members. The triangular shaped arm was later determined to difficult to produce reliably with the available equipment. The specimen was then used to validate the experimental testing procedure. This arm is essentially an enlarged version of the square arm. It can be seen in Figure 62 that this arm failed similar to the square arm.

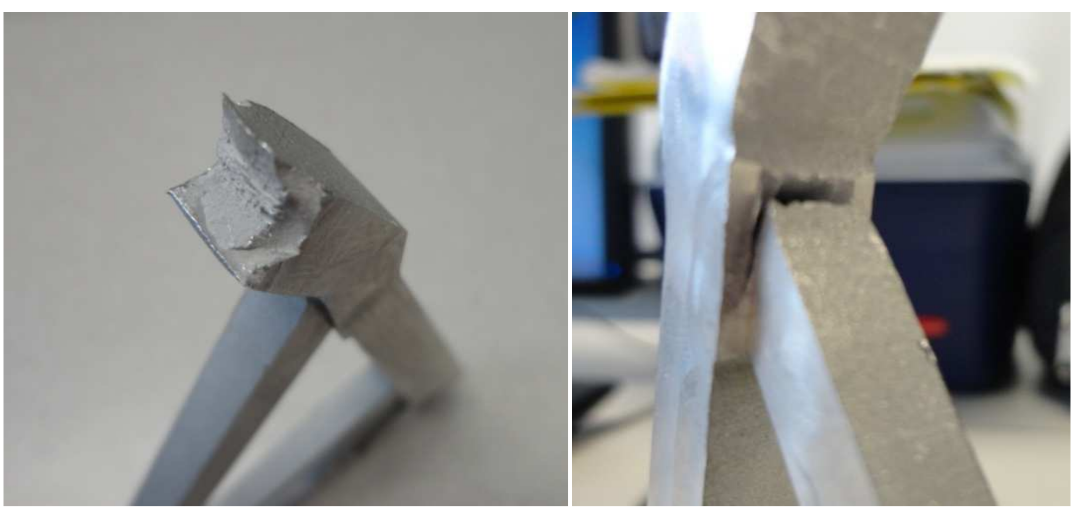

Figure 62 - Triangle Fracture Pre-CNC (Sample Test)

The second sample test piece is what would have become the circular arm. Once again the manufacture of this particular arm was aborted because of the difficulties associated in producing this arm accurately and repeatedly. It can be observed in Figure 63 that this arm had begun undergoing the final machining process. The circle arm was tested in the same manner as was used in the other arms and the triangular sample test specimen. This arm however was not tested until complete failure. The results of this sample test specimen can be compared to that of the circular FEA. It can be seen that the experimental overall deformation of this arm matches closely to that of the FEA study. These two different results agree favorably and warrant credit to the finite element capabilities of the Pro-Engineer software. The buckling nature of the longest bracing member is accurately displayed in the FEA results. It should be noted that if this arm were more easily produced it may provide interesting results.

Figure 63 - Circle Failure (Sample Test)

Lastly, the general results of stage I of this study provided an insight into how the addition of bracing members affects deflections in control arms. It can be observed from the overall results that the addition of bracing does effect the deflections that occur in control arms. It can also be concluded that aluminum control arms can be made to provide results comparable to those made of 1020 steel. Interestingly enough though the addition of bracing did not significantly improve the load which an arm was able to withstand. It only managed to change the nature of failure that occurred in the arms and the location of that failure. It can also be observed that the cross sectional shape of the bracing did affect the maximum deflection that occurred in the arms. The orientation of the shape used will also affect the results as was observed in the comparison of rectangle I and rectangle II. The differences in deflections depending on the shape used were not significant although they were detectable.

During the first stage of this study an arbitrary 'Z' shaped trajectory, for the bracing was used. It is important to note the previous results are likely dependent on that specific orientation of the bracing members. The arms studied in stage I mostly failed at approximately the same location, which was revealed by the FEA. The addition of bracing members was successful in reducing deflections although it created a common failure point among the different arms.

A2 - Stage II Discussion of Failure

During stage II, several different cross sectional shapes were evaluated for their effectiveness in reducing deflections occurring in a control arms. The shapes all followed an arbitrary ‘X’ shaped trajectory. Only the rectangle I arm was manufactured from 6061 aluminum and tested experimentally. This was done in order to provide proof of concept in an actual experiment. Two identical specimen of rectangle I in this stage of the study were manufactured and tested. These arms were inserted into the specially designed testing apparatus and a continually increasing load was applied to the arms until failure occurred. The test was performed the same way as stage I. Each of the two arms failed in the same way and produced nearly identical results.

A2.1 - Rectangle I

The rectangular I arm was tested in an identical manner as the previous arms. The arm was tested until failure occurred; similarly, the strain, load and deflection were monitored continuously. The failed rectangle I arm can be observed in Figure 64 and Figure 65. The testing of this arm was stopped when one of the bracing members completely fractured. This cause the test to terminate because the load being applied decreased by greater than 25% of the maximum load reached for this specimen. As mentioned previously the 25% threshold was a test parameter which was predetermined and programmed into the testing software.

Figure 64 - 'X' Trajectory Rectangle I Cross Section Failure

Both of the samples tested physically during this stage of this study failed identically. It can be observed in Figure 64 that arm utilizing the rectangular I shaped bracing members following the 'X' trajectory failed suddenly by fracturing. The sudden failure ended the test but provided favorable results. As mentioned earlier, the arms utilizing the 'X' trajectory decreased in all areas of focus when compared to the arms from stage I that followed the 'Z' trajectory. That is the maximum von Mises stress, maximum principal strains and the maximum displacements were decreased for each cross sectional shape when compared to same shape following the 'Z' trajectory. The same were decreased when compared to the unbraced aluminum arm. In addition, the 'X' trajectory arms that were tested experimentally withstood a maximum load that was larger than those arms utilizing the 'Z' shaped trajectory. Even with the increased load capacity, the 'X' trajectory arms produced smooth load vs. deflection curves. Additionally when these arms failed, they managed fail in the most desirable of ways. The outer elements of the arms did not fracture and remained intact, making this a desirable configuration.

Figure 65 - 'X' Trajectory Rectangle I Cross Section Fracture

The location of the failure occurring in this arm can be observed in Figure 65. The failed bracing element fractured at the point where it merged with the outer elements of the arm. It can be observed that the other bracing member located in the arm completely buckled and deflected outward, refer to Figure 64. Mentioned earlier was that the 'X' trajectory arm was symmetric which makes universal and applicable to multiple applications. Additionally the arms utilizing an 'X' trajectory are most applicable to current common suspension systems.

ACADEMIC VITA

James Anderson
560 Willow St. Apt. K
Highspire, PA 17034
(570) 952-5850
Janderson0988@yahoo.com

Education

B.S. Mechanical Engineering — August 2011-May 2014
Pennsylvania State University, Harrisburg, PA 17057
Schreyer Honors Student

Lehigh Carbon Community College — August 2007-May 2011
Schnecksville, PA 18078

Employment

5/2013 - 8/2013 Manufacturing Engineer/ Intern
Lockheed Martin Missiles and Fire Control, Camden, AR

- Designed tooling, gauges and shop aids required for production.
- Obtained materials and prepared work orders.
- Wrote work instructions for product manufacturing.

8/2013 - 5/2014 Peer Tutor -Mechanical Engineering, Physics, Mathematics
Pennsylvania State University - Russell E. Horn Learning Center, Harrisburg, PA

- CRLA certified level II tutor
- Help students with any course related issues they may have.

4/2006 - 8/2011 Fleet Mechanic/ Automotive Technician
Pocono Whitewater Rafting, Jim Thorpe, PA

- Performed regulatory maintenance and repairs on more than 60 vehicles, machinery, and mechanical equipment.
- Was responsible for vehicle logistics.

3/2004 - 8/2011 Maintenance and Customer Service
Skirmish USA, Jim Thorpe, PA

- Directed and assisted customers with various issues such as equipment malfunctions and complaints.
- Assisted in development and implementation of an efficient rental equipment distribution and retrieval system. Cut down two thirds of the staffing needs.

Achievements

Undergraduate Thesis – “A Study of Stiffness in Control Arms Utilizing Inner Webbed Structures to Minimize Deflections”
Geothermal Analysis - Pennsylvania State Police Data Center
Schreyer Honors College: Fall 2012 – Spring 2014
Phi Kappa Phi National Honor Society Member
Alpha Sigma Lambda Adult Honor Society Member
NACK workshops – Nanotechnology Seminar Participant
Deans Honors: Summer - 2012; Fall - 2007, 2010, 2011, 2012, 2013; Spring - 2009, 2010, 2012, 2013
South Central Pennsylvania Robotics Competition Judge
Excellence in Automotive Technology Award

Skills

Pro-Engineer	Solid Works	MatLab
Microsoft Office	Fabricating/ Welding	GD&T
CNC Programming	Machining	Manufacturing
Effective Communication		